

Anna Lueger, BSc.

# **Dipeptidyl peptidase 3 in MCF-7 and MDA-MB-231 breast cancer cell lines and its role in oxidative stress**

## **MASTER'S THESIS**

to achieve the university degree of  
Master of Science

Master's degree programme: Biochemistry and Molecular Biomedicine

submitted to

**Graz University of Technology**

### **Supervisors**

Univ.-Prof. Dr.rer.nat. Peter Macheroux

Mag. Grazia Malovan

Institute of Biochemistry, Graz University of Technology

Ass. Prof. Julia Kargl, PhD.

Otto Loewi Research Center, Division of Pharmacology, Medical University of Graz

Graz, January 2022

## **AFFIDAVIT**

I declare that I have authored this thesis independently, that I have not used other than the declared sources/resources, and that I have explicitly indicated all material which has been quoted either literally or by content from the sources used. The text document uploaded to TUGRAZonline is identical to the present master's thesis.

---

Date, Signature

# Acknowledgements

First, I would like to thank my thesis supervisor Univ. Prof. Dr. Peter Macheroux for enabling me to first do my bachelor's thesis and now do my master's thesis in his group at the Institute of Biochemistry at Graz University of Technology. His advice and guidance have been invaluable during my time here and are greatly appreciated. He took the time to listen to my numerous questions and guided me through problems about my research and writing.

At this point I would also like to take the opportunity to thank the members of the biochemistry department for welcoming me to the institute and for always taking the time to help if I had issues with my research.

I would also like to show my sincere gratitude to my supervisor Mag. Grazia Malovan, who has been my teacher and mentor during my studies. Her teaching style and her encouragement has helped me gain confidence in my abilities, and our lively discussions have helped and educated me in many ways. I would like to thank her very much for her ongoing support and for dedicating the time and effort to helping me along my way.

Next, I wish to acknowledge the opportunity to do part of my experiments at the Division of Pharmacology at Medical University of Graz provided by Ass. Prof. Julia Kargl, PhD. I would like to thank her for her insightful feedback and ideas, and I would like to thank the members of her research group for their patient support and assistance.

## Abstract

Due to their high metabolic demand, cancer cells are exposed to increased levels of reactive oxygen species (ROS), and therefore, oxidative stress under basal conditions. Dipeptidyl peptidase 3 (DPP3) has an alleviating effect on oxidative stress as a result of its involvement in the Keap1-Nrf2-ARE pathway. In cancer, for instance in breast cancer, high expression of *Dpp3* can lead to better survival of cancer cells, and therefore, correlates with poor prognosis. Although DPP3 is a cytoprotective protein that supports the antioxidant system in cells, the presence of DPP3 can have beneficial or harmful effects depending on the pathological condition. The purpose of this thesis was to investigate the importance of DPP3 in breast cancer and to explore the response of breast cancer cells to oxidative stress.

Toward this aim, the breast cancer cell lines MCF-7 and MDA-MB-231 were exposed to hyperoxia and studied through qPCR, western blot, immunofluorescence, cell fractionation, ROS and H<sub>2</sub>O<sub>2</sub> measurements as well as several assays, such as the MTT-, TBARS, AnnexinV/PI and the DPP3 activity assay. I could demonstrate that in MDA-MB-231 cells *Dpp3* transcript levels can be induced through oxidative stress and that this increase in *Dpp3* correlates with survival of cells, as they do not show signs of apoptosis after hyperoxia treatment. This result further supports the hypothesis that DPP3 is cytoprotective and alleviates oxidative stress. Also, I report that the MCF-7 and the MDA-MB-231 cell lines show no cell damage or increase in ROS levels indicating an effective defense of these cell lines against oxidative stress. Furthermore, I show that DPP3 is localised in the nucleus through immunofluorescence and is independent of oxidative stress. I also detected DPP3 in the nucleus through western blot, however, this should be further analysed as I could not assess the purity of the nuclear fractions in this experiment. To better understand the localization of DPP3 and its potential as a marker for prognosis in cancer or as a target for cancer therapy, further studies are necessary.

## Zusammenfassung

Aufgrund ihres hohen Stoffwechselbedarfs sind Krebszellen unter basalen Bedingungen erhöhten Mengen an reaktiven Sauerstoffspezies (ROS) und damit oxidativem Stress ausgesetzt. Dipeptidylpeptidase 3 (DPP3) hat aufgrund seiner Mitwirkung am Keap1-Nrf2-ARE System eine reduzierende Wirkung auf oxidativen Stress. Bei Krebs, beispielsweise Brustkrebs, kann eine hohe Expression von *Dpp3* zu einem besseren Überleben von Krebszellen führen und korreliert daher mit einer schlechter Prognose. Obwohl DPP3 ein zytoprotektives Protein ist, das das anti-oxidative System in Zellen unterstützt, kann das Vorhandensein von DPP3 je nach pathologischem Zustand vorteilhafte oder nachteilige Wirkungen haben. Ziel dieser Arbeit war es, die Bedeutung von DPP3 in Brustkrebs zu untersuchen und die Reaktion von Brustkrebszellen auf oxidativem Stress zu untersuchen. Die Brustkrebszelllinien MCF-7 und MDA-MB-231 wurden Hyperoxie ausgesetzt und durch qPCR, Western Blot, Immunfluoreszenz, Zellfraktionierung, Bestimmung von ROS und H<sub>2</sub>O<sub>2</sub> sowie verschiedener Nachweismethoden wie die MTT-, AnnexinV/PI- und TBARS Bestimmung untersucht. Ich konnte zeigen, dass in MDA-MB-231-Zellen die *Dpp3* mRNA Menge durch oxidativen Stress erhöht werden kann und dass dieser Anstieg von *Dpp3* mit dem Überleben der Zellen korreliert, da sie nach der Hyperoxie Behandlung keine Anzeichen von Apoptose zeigen. Dieses Ergebnis stützt weiter die Hypothese, dass DPP3 zytoprotektiv ist und oxidativen Stress reduziert. Außerdem berichte ich, dass die Zelllinien MCF-7 und MDA-MB-231 keine Zellschädigung oder Erhöhung der ROS aufweisen, was auf eine effektive Abwehr dieser Zelllinien gegen oxidativen Stress hinweist. Darüber hinaus zeige ich durch Immunfluoreszenz, dass DPP3 im Zellkern lokalisiert ist und die Lokalisierung nicht unmittelbar von oxidativem Stress abhängt. Ich habe DPP3 im Zellkern auch durch Western Blot nachgewiesen, dies sollte jedoch genauer untersucht werden, da in diesem Experiment die Reinheit der Kernfraktion nicht beurteilt werden konnte. Um die Lokalisation von DPP3 und das Potenzial von DPP3 als Marker für eine Prognose bei Krebserkrankungen oder als Angriffspunkt für mögliche Krebstherapien besser zu verstehen sind weitere Experimente notwendig.

# Table of contents

Acknowledgements .....	I
Abstract .....	II
Zusammenfassung .....	III
Table of contents .....	IV
List of Figures .....	VI
List of Tables .....	VI
Abbreviations .....	VII
<b>1. Introduction.....</b>	<b>1</b>
1.1. Dipeptidyl peptidase 3.....	1
1.2. DPP3 and oxidative stress.....	3
1.3. Oxidative stress in cancer.....	7
1.4. Aim of this project .....	9
<b>2. Material and methods.....</b>	<b>10</b>
2.1. Cell culture .....	10
2.2. Conditions of hyperoxia .....	10
2.3. Quantitative PCR .....	10
2.3.1. RNA Isolation.....	10
2.3.2. cDNA reverse transcription.....	11
2.3.3. qPCR .....	11
2.4. Protein isolation, SDS-Page and western blotting .....	11
2.5. DPP3 activity assay .....	12
2.6. Isolation of subcellular fractions .....	12
2.7. Immunofluorescence .....	13
2.8. Cell viability – MTT assay.....	14
2.9. ROS production.....	14
2.10. Quantitative peroxide assay (H <sub>2</sub> O <sub>2</sub> assay).....	14
2.11. Determination of lipid peroxidation using TBARS (thiobarbituric acid reactive substances) assay....	15
2.12. AnnexinV and PI apoptosis assay .....	15
2.13. Programs and statistics .....	15
<b>3. Results .....</b>	<b>16</b>
3.1. Characterization of DPP3 in MCF-7 and MDA-MB-231 cell lines .....	16
3.1.1. <i>Dpp3</i> transcript levels after hyperoxia treatment .....	16
3.1.2. <i>Dpp3</i> protein expression after hyperoxia treatment .....	17
3.1.3. DPP3 activity after hyperoxia treatment .....	17
3.2. Localization of DPP3 in MCF-7 and MDA-MB-231 cells .....	18
3.2.1. Immunofluorescence .....	18
3.2.2. <i>Dpp3</i> protein expression in cytosolic and nuclear fractions.....	19

3.2.3.	DPP3 activity assay in cytosolic and nuclear fractions .....	20
3.3.	Characterization of MCF-7 and MDA-MB-231 cell lines after hyperoxia treatment .....	21
3.3.1.	Analyzing NAD(P)H availability with MTT assay.....	21
3.3.2.	Expression of ARE proteins after hyperoxia treatment.....	22
3.3.1.	Total ROS production after hyperoxia treatment.....	23
3.3.1.	Hydrogen peroxide concentration after hyperoxia treatment.....	23
3.3.1.	Lipid peroxidation after hyperoxia.....	24
3.3.1.	Analysis of apoptosis with AnnexinV/PI assay .....	25
4.	<b>Discussion.....</b>	<b>26</b>
5.	<b>References.....</b>	<b>32</b>
6.	<b>Supplementary data.....</b>	<b>40</b>

## List of Figures

Figure 1: Structure of human DPP3 .....	1
Figure 2: Creation of reactive oxygen species .....	4
Figure 3: Involvement of DPP3 in the Keap1-Nrf2-ARE pathway .....	5
Figure 4: Analysis of mRNA levels of <i>dpp3</i> using qPCR in MCF-7 and MDA-MB-231 cell lines .....	16
Figure 5: Analysis of DPP3 protein expression using western blot in MCF-7 and MDA-MB-231 cell lines.....	17
Figure 6: Enzyme specific activity of DPP3 in MCF-7 and MDA-MB-231 cell lines.....	18
Figure 7: Immunofluorescence analysis of DPP3 in MCF-7 and MDA-MB-231 cell lines....	19
Figure 8: Expression of <i>Dpp3</i> in cytosolic and nuclear fractions of MCF-7 and MDA-MB-231 cell lines.....	20
Figure 9: DPP3 activity in cytosolic and nuclear fractions of MCF-7 and MDA-MB-231 cell lines .....	20
Figure 10: Analysis of NAD(P)H availability using MTT assay in MCF-7 and MDA-MB-231 cell lines.....	21
Figure 11: Protein expression of the ARE genes SOD2, NQO1 and HO-1 in MCF-7 and MDA-MB-231 cell lines. ....	22
Figure 12: Total ROS production after hyperoxia treatment in MCF-7 and MDA-MB-231 cell lines .....	23
Figure 13: Hydrogen peroxide concentration after hyperoxia treatment in MCF-7 and MDA-MB-231 cell lines .....	24
Figure 14: Analysis of lipid peroxidation by TBARS assay in MCF-7 and MDA-MB-231 cell lines .....	24
Figure 15: Analysis of apoptosis with AnnexinV/PI apoptosis assay in MCF-7 and MDA-MB-231 cell lines.....	25

## List of Tables

Table 1: Primary and secondary antibodies used for western blot.....	12
Table 2: Buffers for isolation of subcellular fractions .....	13
Table 3: Primary and secondary antibodies used for immunofluorescence.....	14



## Abbreviations

ARE	antioxidant response elements
CDK1	cyclin-dependent kinase 1
DAPI	4',6-Diamidino-2-phenylindol
DNA	deoxyribonucleic acid
DPP3	dipeptidyl-peptidase 3
FITC	fluorescein isothiocyanate
GAPDH	Glyceraldehyd-3-phosphat-Dehydrogenase
GSH	glutathione
H <sub>2</sub> DCFDA	2',7'- dichlorodihydrofluorescein diacetate
HO-1	heme oxygenase 1
Keap1	kelch-like ECH-associated protein 1
MDA	malondialdehyde
MTT	3-(4,5-dimethylthiazol-2-yl)-2,5-diphenyltetrazolium bromide
NADH	nicotinamide adenine dinucleotide
NADPH	nicotinamide adenine dinucleotide phosphate
NLS	nuclear localization signal
NPC	nuclear pore complex
NQO1	NAD(P)H quinone dehydrogenase 1
Nrf2	nuclear factor erythroid 2-related factor 2
OGD/R	oxygen-glucose deprivation/reoxygenation
p21	cyclin-dependent kinase inhibitor 1
p53	tumor protein p53
PBS	phosphate-buffered saline
PI	propidium iodide
RAS	renin-angiotensin system
ROS	reactive oxygen species
Small Maf	musculoaponeurotic fibrosarcoma
SOD2	superoxide dismutase
TBARS	thiobarbituric acid reactive substances
TNA- $\alpha$	tumor necrosis factor alpha

# 1. Introduction

## 1.1. Dipeptidyl peptidase 3

Dipeptidyl peptidase 3 (DPP3), a member of the M49 metallopeptidase family, is a zinc-dependent aminopeptidase that cleaves dipeptides sequentially from the N-terminus of oligopeptides (Kaufmann et al., 2019; Prajapati & Chauhan, 2011). First isolated in 1967 from bovine pituitary, the two-lobed protein has an approximate molecular weight of 82 kDa and has since been isolated from various organisms from bacteria to higher eukaryotes (Baršun et al., 2007; Ellis & Nuenke, 1967; Jha et al., 2020; Kaufmann et al., 2019). DPP3 is expressed in multiple tissues in mammals, including erythrocytes, brain, skin, kidney, liver and spinal cord (Kumar et al., 2016). It was also found to be part of the human proteome and is expressed in all human cells ubiquitously (Jha et al., 2020). The protein has a two-lobed structure with a wide cleft in between, where the catalytic zinc-ion is located (Figure 1) and has a unique HEXXGH motif in the upper lobe (Baral et al., 2008). The upper lobe that contains the catalytically relevant residues is mostly made of alpha helices. It is connected to the lower lobe, which is made of both alpha helices and beta sheets, by multiple flexible loops (Baral et al., 2008). When binding a peptide, DPP3 undergoes a conformational change, forming the closed structure independent from the nature of the peptide (Kumar et al., 2016).

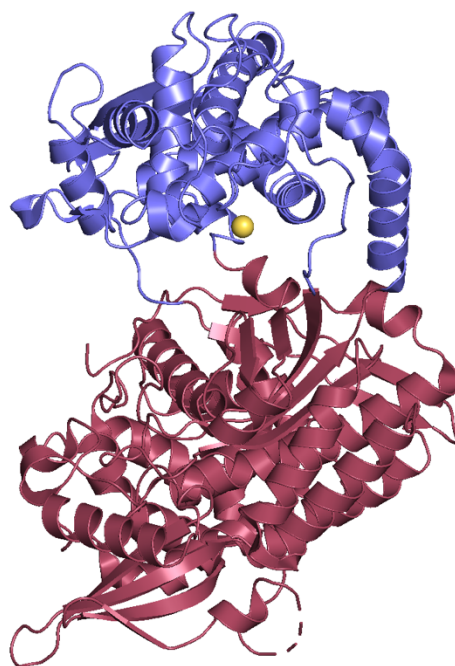


Figure 1: Structure of human DPP3 (PDB: 3FVY). DPP3 is a two lobed protein, which consists of both alpha helices and beta sheets. The upper lobe is shown in blue, the lower lobe in red and the zinc ion in the cleft is shown as a yellow sphere. The structure is shown in open conformation when no substrate is bound. This structure was prepared using PyMOL ([www.pymol.org](http://www.pymol.org))

DPP3 has been described as a cytosolic protein (Grdiša & Vitale, 1991; Ohkubo et al., 2000), although some research suggests localization of DPP3 in the nucleus (Mačak Šafranko et al., 2015; Sobočanec et al., 2016), while other research suggests its association with membranes (Mazzocco et al., 2006; Prajapati & Chauhan, 2011). With a size of approximately 82 kDa, it is highly unlikely that DPP3 is translocated into the nucleus via passive diffusion, as proteins that are larger than 40 kDa already have difficulties diffusing into the nucleus (Cautain et al., 2015; Fried & Kutay, 2003). There is also no report of DPP3 having a nuclear localization signal (NLS), which is one of the requirements for active transport through the nuclear pore complex into the nucleus (Fried & Kutay, 2003). The NLS of a cytosolic protein is recognized by importin proteins, and the transport through the nuclear pore complex (NPC) is facilitated (Cautain et al., 2015; J. Lu et al., 2021). Further mechanisms of nuclear import include the use of calcium-binding proteins that can directly interact with the NPC and act as protein carriers (Cautain et al., 2015; Wagstaff & Jans, 2009). An additional way to enter the nucleus for proteins without a NLS sequence is the “piggyback” mechanism, where proteins are imported into the nucleus when they interact with proteins that have a functional NLS sequence (Cautain et al., 2015). Although there are multiple ways for proteins to translocate into the nucleus, it is unknown how DPP3 might translocate into the nucleus.

DPP3 seems to be involved in physiological and pathological processes such as inflammation (Menale et al., 2019; Ren et al., 2021), blood pressure regulation (Deniau et al., 2019; Jha et al., 2020; Rehfeld et al., 2019; Takagi et al., 2019), pain modulation (Hashimoto et al., 2000), oxidative stress (Liu et al., 2007; Menale et al., 2019; Ren et al., 2021) and cancer (Hast et al., 2013; Lu et al., 2017). For instance, DPP3 was linked to blood pressure regulation and pain modulation because of its high affinity for angiotensin II, angiotensin III and enkephalins (Jha et al., 2020; Pang et al., 2016). Angiotensin II is part of the renin-angiotensin system (RAS) and is among others responsible for the elevation of blood pressure, which is why angiotensin II receptor blockers are used to treat hypertension (Pang et al., 2016). An in-vivo study with mice showed that the effect of DPP3-injection was similar to the treatment with an angiotensin II receptor blocker (Pang et al., 2016). DPP3 shows a high affinity for angiotensin II and cleaves it efficiently, which shows the potential of DPP3 in treatment against hypertension (Pang et al., 2016).

Research also suggests the involvement of DPP3 in the alleviation of oxidative stress and inflammation through the Keap1-Nrf2-ARE pathway (Lu et al., 2017), which is an important defense mechanism against oxidative stress (Lee & Hu, 2020; Taguchi & Yamamoto, 2017). This involvement was shown in *Dpp3*-knockout mice, which experience more oxidative stress,

growth defect and increased bone loss (Menale et al., 2019). Furthermore, in oxygen-glucose deprivation/reoxygenation injured (OGD/R-injured) neurons, the presence of DPP3 suppresses apoptosis, oxidative stress and inflammation as a result of the Keap1-Nrf2-ARE pathway (Ren et al., 2021).

In addition, overexpression of *Dpp3* has been found in breast cancer (Lu et al., 2017), ovarian cancer (Šimaga et al., 2003) and lung cancer (Hast et al., 2013) and has been linked with poor prognosis in multiple studies (Lu et al., 2017; Tong et al., 2021). Research in colorectal cancer suggests that DPP3 interacts with CDK1, its downregulation leading to inhibition of cell proliferation, and concludes that DPP3 has oncogene-like functions (Tong et al., 2021). In breast cancer *Dpp3* seems to be overexpressed, which correlates with poor prognosis in ER+ breast cancer patients. This was explained due to the elevating effect DPP3 has on nuclear erythroid 2-related factor 2 (Nrf2), and its resulting antioxidant effect, as oxidative stress functions as a barrier of metastasis (Lu et al., 2017). This correlation between high expression of *Dpp3* and poor prognosis in cancer makes DPP3 an interesting research objective in cancer studies. DPP3 has been proposed as a potential marker and target for cancer prognosis and treatment in various studies (Lu et al., 2017; Tong et al., 2021).

In summary, whereas DPP3 suppresses oxidative stress and related diseases such as hypertension, DPP3 is also linked to poor prognosis in cancer studies (Lu et al., 2017) and has even been described as oncogene-like (Tong et al., 2021). Current research demonstrates that DPP3 may have a positive as well as a negative impact on pathological conditions, as its effect to alleviate oxidative stress has different consequences depending on the condition. The biological function of DPP3 is therefore not well understood.

## **1.2. DPP3 and oxidative stress**

Oxidative stress can be described as the accumulation of commonly occurring reactive oxygen species (ROS) compounds, which is caused by an imbalance between ROS production and anti-oxidative defense in the cells (Menale et al., 2019). This accumulation of molecules such as superoxide anion ( $\bullet\text{O}_2^-$ ), hydroxyl radical ( $\bullet\text{OH}$ ), and hydrogen peroxide ( $\text{H}_2\text{O}_2$ ) can lead to damage of biomolecules like DNA, proteins and lipids in the cells (Ray et al., 2012). The production of these potentially damaging ROS occurs during electron transfer reactions (Thannickal & Fanburg, 2000), such as the oxidative phosphorylation in mitochondria of cells (Figure 2), where ROS are created as by-products (Thannickal & Fanburg, 2000; Zhang et al., 2016).

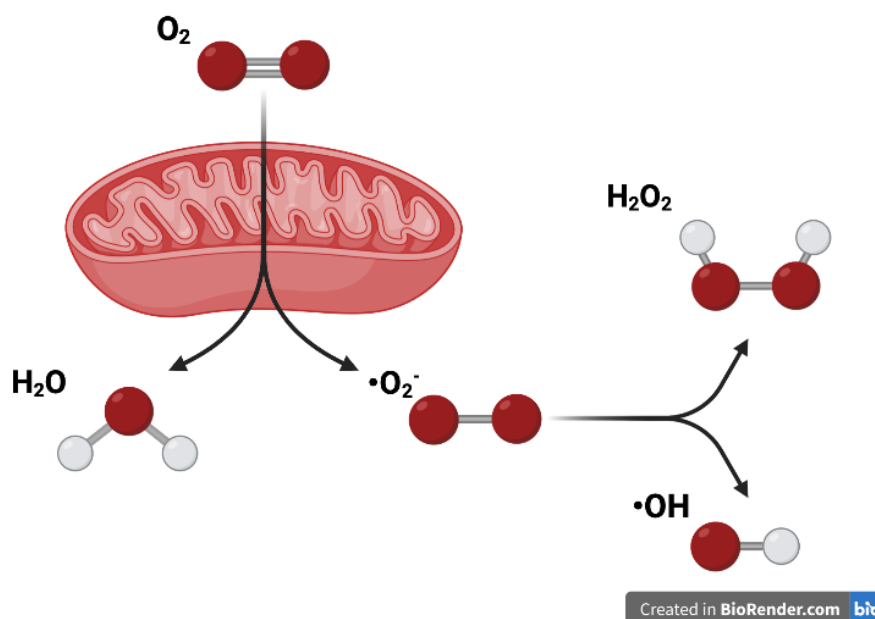


Figure 2: Creation of reactive oxygen species. In processes like the oxidative phosphorylation, molecules such as superoxide anion ( $O_2^-$ ), hydroxyl radical ( $\cdot OH$ ), and hydrogen peroxide ( $H_2O_2$ ) are produced as a byproduct of oxidative phosphorylation in mitochondria (Thannickal & Fanburg, 2000). The image was created with BioRender.com

Although the accumulation of ROS in cells can have a damaging effect, ROS also has functions as cell signaling molecules (Zhang et al., 2016) and are a part of the innate immune response as they have antimicrobial activities (Day, 2019). Furthermore, normal levels of ROS are known to promote cell proliferation (Weinberg et al., 2010) and transcriptional activation (Ray et al., 2012). The excessive buildup of free radicals leads to genomic instability by causing DNA damage (Srinivas et al., 2019), and therefore promotes tumor initiation and in some cases tumor metastasis (Ray et al., 2012; Srinivas et al., 2019; Weinberg et al., 2010). In cancer cells, ROS levels seem to be higher than in normal cells and the cancer cells show an increased antioxidant mechanism (Gorrini et al., 2013). As ROS is involved in the regulation of proliferation (Weinberg et al., 2010), apoptosis (Ray et al., 2012) and tumorigenesis (Srinivas et al., 2019; Weinberg et al., 2010), researchers are constantly developing therapeutic strategies to treat or prevent ROS mediated diseases (Ray et al., 2012).

To balance the endogenous production of ROS, multiple antioxidant enzymes are expressed by cells. These enzymes include proteins such as superoxide dismutase (SOD2) and NAD(P)H quinone dehydrogenase 1 (NQO1), proteins which scavenge superoxide, and the anti-inflammatory protein heme oxygenase 1 (HO-1) (Tu et al., 2019). These proteins are part of the antioxidant response element (ARE), a sequence in the DNA that codes for several cytoprotective proteins (Lee & Hu, 2020; Raghunath et al., 2018; Taguchi & Yamamoto, 2017).

The transcription of these antioxidant genes is regulated through the Keap1-Nrf2-ARE pathway (Lee & Hu, 2020; Raghunath et al., 2018; Taguchi & Yamamoto, 2017). Under basal conditions, Kelch-like ECH-associated protein 1 (Keap1) binds Nrf2 and leads to the ubiquitination and degradation of Nrf2 (Taguchi & Yamamoto, 2017). The binding to Keap1 is enabled by the ETGE and DLC motif of Nrf2 and it is structured as a trimer of one Keap1-homodimer and a single Nrf2 molecule (Lee & Hu, 2020; Taguchi & Yamamoto, 2017). The binding leads to degradation of Nrf2 through the 26S proteasome and thereby hinders Nrf2 from translocating into the nucleus to activate transcription of antioxidant genes (Taguchi & Yamamoto, 2017; Tu et al., 2019). Other proteins that have the ETGE motif or ETGE-like binding motifs, including DPP3, can also bind to Keap1 and thereby compete with Nrf2 (Lu et al., 2017).

The involvement of DPP3 in the defense of oxidative stress was linked to the Keap1-Nrf2 antioxidant pathway in multiple studies (Hast et al., 2013; Lu et al., 2017; Menale et al., 2019; Ren et al., 2021). DPP3 can bind Keap1 through its ETGE motif and therefore acts like a competitor to Nrf2 (Figure 3) (Lu et al., 2017).

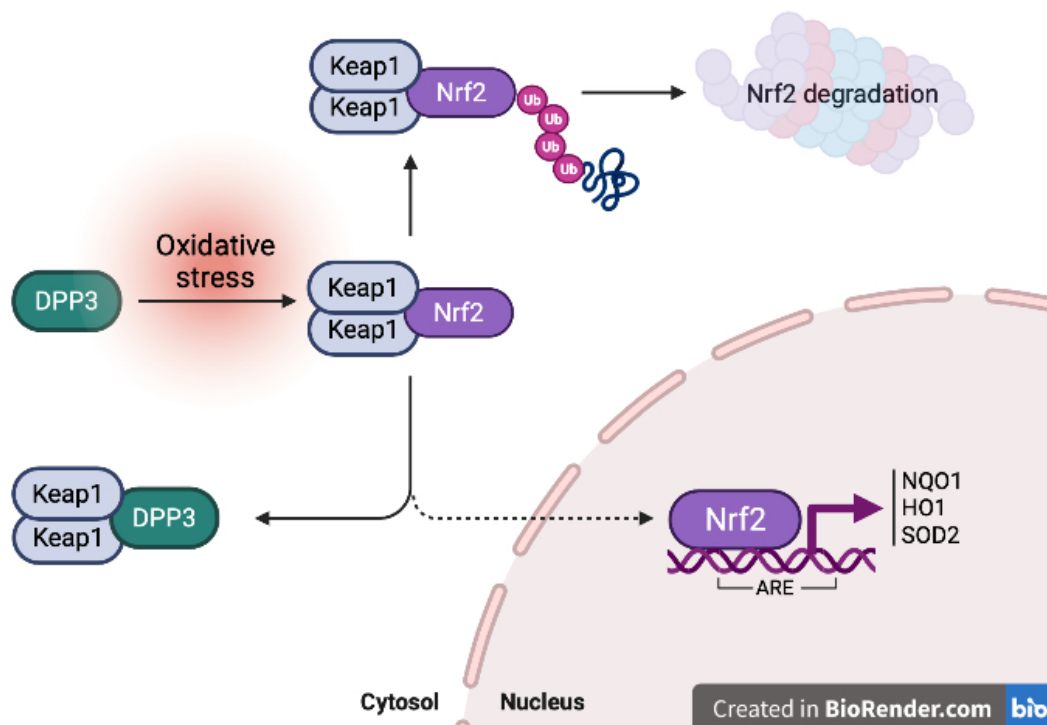


Figure 3: Involvement of DPP3 in the Keap1-Nrf2-ARE pathway. In physiological conditions, Nrf2 binds to Keap1, leading to the ubiquitination and degradation by the 26Sproteasome of Nrf2 (Taguchi & Yamamoto, 2017). DPP3 can bind to Keap1 competitively and therefore promote the translocation of Nrf2 to the nucleus (Lu et al., 2017). In the nucleus, Nrf2 acts as a transcription factor for the ARE genes, promoting the antioxidant response by increasing expression of NQO1, HO-1 and SOD2 (Taguchi & Yamamoto, 2017). The image was created with BioRender.com

This means Nrf2 can dissociate from Keap1 and translocate to the nucleus, where it acts as a transcription factor for the ARE. Together with musculoaponeurotic fibrosarcoma (small Maf) proteins, Nrf2 binds to the ARE sequence and leads to their transcription (Taguchi & Yamamoto, 2017). The transcription is therefore activated by Nrf2, and cytoprotective proteins like NQO1 and HO-1 can counteract the accumulation of ROS and therefore prevent cell damage (Taguchi & Yamamoto, 2017; Tu et al., 2019).

This interaction of DPP3 with the Keap1-Nrf2-ARE pathway has been shown to be relevant in multiple pathological conditions (Hast et al., 2013; Menale et al., 2019; Ren et al., 2021). *Ren et al* have found in their research with oxygen-glucose deprivation/reoxygenation injured (OGD/R-injured) neurons, that DPP3 binds to Keap1 and therefore leads to more Nrf2 translocating to the nucleus and to a better antioxidant response (Ren et al., 2021). They show that by this process DPP3 suppresses apoptosis, oxidative stress and inflammation and conclude that DPP3 is neuroprotective in OGD/R-injured neurons (Ren et al., 2021).

A similar positive effect of DPP3 could be seen in *Dpp3*-knock out mice, which experience more oxidative stress than mice with DPP3 protein expression. The DPP3-depleted osteoclasts showed increased ROS production, which led to higher probability of apoptosis (Menale et al., 2019). In both breast cancer (Lu et al., 2017) and lung cancer cells (Hast et al., 2013), overexpressed *Dpp3* was linked to an increase in the Nrf2-dependend transcription of the ARE genes. These studies support the relevance of DPP3 in oxidative stress and its potentially positive effect in some pathological conditions.

The proteins of the ARE are extremely important for the cellular defense against oxidative stress. The manganese dependent enzyme SOD2 is substantial for the scavenging of superoxide in response to oxidative stress (Dewaele et al., 2010; Portakal et al., 2000). SOD2 is primarily located in the mitochondria of cells and converts superoxide to hydrogen peroxide (Portakal et al., 2000). In multiple cancers, including breast cancer (Portakal et al., 2000) and pancreas cancer (Hurt et al., 2007) the activity of SOD2 is altered. Increase of SOD2 activity indicates better survival of cancer cells (Dhar & st. Clair, 2012; Portakal et al., 2000). Furthermore, NQO1 is a flavoprotein which reduces molecules such as quinones and nitroaromatics, and the reduction that is catalyzed by NQO1 is dependent on NAD(P)H acting as an electron donor (Dinkova-Kostova & Talalay, 2010). NQO1 is also enabled to scavenge superoxide directly, adding to its cytoprotective role and research even suggests an impact of NQO1 on the ratios of reduced/oxidized pyridine nucleotides (NADPH/NADP<sup>+</sup>) (Dinkova-Kostova & Talalay, 2010). Heavily induced by oxidative stress, HO-1 is both an antioxidant and anti-inflammatory enzyme (Dennery, 2014; Tu et al., 2019). It degrades heme to the antioxidant pigment biliverdin

and signaling molecules like carbon monoxide (Tu et al., 2019), aiding the response against oxidative stress as the resulting bile pigments are highly antioxidant. Moreover, HO-1 also has a nonenzymatic role as a signaling molecule, regulating proteins that show importance for the repair of damaged DNA (Dennerly, 2014).

To sum up, the involvement of DPP3 in the defense against oxidative stress was shown in multiple studies and its effect seems to be cytoprotective. By binding to Keap1, DPP3 leads to a higher expression of the ARE genes and by therefore helps to protect the cell against oxidative stress (Lu et al., 2017). The protection against free radicals in cells leads to better cell survival, preventing apoptosis (Ren et al., 2021). This cytoprotective function of DPP3 is not always favorable, since in some cancers *Dpp3* is overexpressed (Lu et al., 2017; Šimaga et al., 2003), resulting in better survival of cancer cells and poor prognosis (Hast et al., 2013; Lu et al., 2017; Ren et al., 2021).

### **1.3. Oxidative stress in cancer**

It was believed that mitochondrial function is inconsequential in cancer cells, as they are said to uptake glucose to use for cell metabolism, which is referred to as the Warburg effect (Vasan et al., 2020; Warburg, 1956). This implies that cancer cells therefore do not rely on oxygen intake (Vasan et al., 2020). In multiple, newer studies the importance of the mitochondrial metabolism was shown, as it seems to be an essential process in tumor growth (Vasan et al., 2020). The metabolism of cancer cells differs in a lot of aspects from normal cells, as they need to adjust to the increased bioenergetic and biosynthetic demand (Martínez-Reyes & Chandel, 2021).

In small quantities, ROS has an important role in signal transduction (Zhang et al., 2016) and transcription (Ray et al., 2012), but higher levels of ROS increase the risk of ROS causing DNA damage, leading to mutations in genes such as p53 and therefore causing tumor development (Srinivas et al., 2019). Several cancer cells show intrinsic oxidative stress, as they produce more superoxide and hydrogen peroxide than normal cells due to their increased metabolism (Martínez-Reyes & Chandel, 2021; Tong et al., 2015). Moreover, those higher levels of ROS in cancer cells are counteracted by upregulating antioxidant proteins in comparison to normal cells, and by supporting NADPH and GSH production (Martínez-Reyes & Chandel, 2021). This implies better cell survival during oxidative stress, as in some cancers antioxidant scavenging is elevated, protecting the cancer cells (Kim et al., 2017; Martínez-Reyes & Chandel, 2021; Saeidnia & Abdollahi, 2013). The relationship between oxidative stress and cancer therefore seems to vary in different cancers and cannot be generalized easily.



The antioxidant enzyme SOD2 has been linked with tumor progression in cancer (Portakal et al., 2000), as it regulates mitochondrial oxidants like  $O_2^-$  and  $H_2O_2$  (Portakal et al., 2000). It was shown that the protein acts as a tumor suppressor in early tumor development and accelerates tumor progression during metastasis (Kim et al., 2017). This dichotomous regulation of the antioxidant enzyme further shows the complexity of antioxidants in cancer (Kim et al., 2017). The effect of oxidative stress on cancer development differs, as in some conditions free radicals can act as cancer inhibitors and in other conditions they act as cancer accelerators (Kim et al., 2017; Saeidnia & Abdollahi, 2013; Sayin et al., 2014). For instance, damage of free radicals to DNA can lead to p53/p21 induction and reduce cell growth (Saeidnia & Abdollahi, 2013; Srinivas et al., 2019), but if DNA repair enzymes are damaged, the effect can be the opposite and cause tumor progression instead (Srinivas et al., 2019). The damage to lipids and inflammation can lead to an increase in inflammatory cytokines such as tumor necrosis factor alpha (TNA- $\alpha$ ), again causing either tumor progression or arrest of cell growth (Saeidnia & Abdollahi, 2013).

This uncertain role of antioxidants in cancer growth leads to multiple strategies in the use of antioxidants as anticancer drugs during chemotherapy (Dewaele et al., 2010; Saeidnia & Abdollahi, 2013). Some antioxidants, such as vitamin C or tetrandrine, are used as anticancer drugs alongside chemotherapy for their ROS scavenging activities (Saeidnia & Abdollahi, 2013; Tong et al., 2015). Due to clinical trials that showed not only an anticancer, but also a cancerogenic effect of antioxidants, some oncologists do not recommend the intake of antioxidants during chemotherapy (Saeidnia & Abdollahi, 2013). Some research even suggests suppressing the antioxidant response to decrease resistance to chemotherapy (Ju et al., 2015; Srinivas et al., 2019). Another strategy to attack cancer cells is to induce apoptosis through ROS accumulation in the cancer cells using compounds like arsenic trioxide or methoxy estradiol (Gupta et al., 2012; Saeidnia & Abdollahi, 2013).

Research regarding the involvement of oxidative stress in cancer and the possible usage of antioxidants in anticancer therapies is still ongoing and a highly relevant research issue.

## 1.4. Aim of this project

Current research shows the possibilities of dipeptidyl peptidase 3 (DPP3) as a potential cancer marker or as a target for cancer treatment (Lu et al., 2017; Tong et al., 2021). DPP3 is involved in an important defense mechanism against oxidative stress, the Keap1-Nrf2-ARE pathway (Lu et al., 2017; Menale et al., 2019; Ren et al., 2021), and the protein seems to mostly have cytoprotective functions (Hast et al., 2013; Lu et al., 2017; Ren et al., 2021). As this cytoprotective function of DPP3 also leads to better survival of cancer cells (Hast et al., 2013; Lu et al., 2017), DPP3 remains an interesting research object in cancer studies.

The aim of this project is to explore the function of DPP3, especially in its role against oxidative stress. Therefore, the plan was to create *Dpp3*-knockout cell lines, induce oxidative stress via hyperoxia and investigate the differences between cells with *Dpp3* expression and *Dpp3*-knockout cells. In the course of the practical work, we were not able to create a stable knockout cell line and had to change the original plan.

We investigated if, in two breast-cancer cell lines, MCF-7 and MDA-MB-231, induction of oxidative stress influences the expression, activity or localization of DPP3.

Furthermore, we wanted to investigate the localization of DPP3 and its possible translocation to the nucleus, as some research suggested this translocation under conditions of oxidative stress (Mačák Šafranko et al., 2015; Sobočanec et al., 2016). As there is no report of DPP3 having a nuclear localization signal and diffusion into the nucleus of such a big protein is highly unusual (Fried & Kutay, 2003; Wagner et al., 1990), we wanted to investigate the localization of DPP3 ourselves.

We also investigated the overall effect of oxidative stress on the breast cancer cell lines regarding their defense against oxidative stress by looking for markers of oxidative stress, cell damage and at the cell viability. To observe an effect of oxidative stress, the cells were treated with oxygen to create hyperoxia conditions and were compared to cells cultured under normal conditions.

## **2. Material and methods**

### **2.1. Cell culture**

The breast cancer cell lines MCF-7 (Cat.no.: ECACC 86012803, Public Health, England) and MDA-MB-231 (Cat.no.: ECACC 92020424, Public Health, England) were used for all experiments. The cells were cultured in DMEM (Dulbecco's modified Eagle's medium, ThermoFisher, USA) supplemented with 10% fetal bovine serum and 1% Penicillin-Streptomycin and were grown in an incubator at 37°C with 5% CO<sub>2</sub> in humid atmosphere.

### **2.2. Conditions of hyperoxia**

All experiments were performed in triplicates equally with a control group and a treated group (hyperoxia). MCF-7 and MDA-MB-231 cells were exposed to hyperoxia for 48 hours in a gas-tight incubator chamber (Modular Incubator Chamber, Billups-Rothenberg, Inc., USA) in an incubator at 37°C in humid atmosphere to induce oxidative stress. For this, cells were seeded overnight at normal conditions in an incubator at 37°C and 5% CO<sub>2</sub> in humid atmosphere. Then the cells were placed in the chamber (hyperoxia), exposed to 95% oxygen for 5 minutes and the gas-tight chamber was sealed and placed in the incubator at 37°C in humid atmosphere. After 24 hours of the treatment, the gas-tight chamber was refilled with 95% O<sub>2</sub> to ensure stability of the treatment. As a control group the same number of cells was seeded overnight and grown for 48 hours under normal conditions in an incubator at 37°C and 5% CO<sub>2</sub> in humid atmosphere.

### **2.3. Quantitative PCR**

#### **2.3.1. RNA Isolation**

To isolate the RNA from the cells,  $2.5 \times 10^5$  cells were seeded in duplicates on a 6-well plate and treated with hyperoxia for 48 hours. The RNeasy Mini Kit from Qiagen (Qiagen, Germany) was used to isolate the RNA. First, 10  $\mu$ l  $\beta$ -mercaptoethanol was added to 1 ml of RLT buffer, and 250  $\mu$ l of this RLT buffer were added to each well. The cells were then detached with a cell scraper and the cell lysate was transferred to Eppendorf tubes. One volume (500  $\mu$ l) of 70% Ethanol was added to the lysate and the lysate was mixed by resuspending. The lysate was transferred to a spin column and centrifuged at 8000g for 30 seconds at 4°C. The flow through was discarded, 700  $\mu$ l RW1 buffer was added to the spin column and the column was centrifuged at 8000 g for 30 seconds at 4°C. After discarding the flowthrough 500  $\mu$ l of RPE buffer was added to the spin column and it was centrifuged again at 8000 g for 30 seconds at 4°C. The flowthrough was discarded and 500  $\mu$ l of RPE was added and centrifuged at 8000

g for 2 minutes at 4°C. The spin column was placed in a new collection tube and centrifuged at 8000g for 1 minute at 4°C to dry. Then the spin column was placed into a new 1.5 ml collection tube, 30 ul of RNase free water was added and the column was centrifuged at 8000 g for 1 minute at 4°C to elute the RNA.

The concentration of the RNA-samples was measured at Nanodrop and the concentration, the ratio 260/280 and the ratio 260/230 was noted for calculation.

### **2.3.2. cDNA reverse transcription**

For the cDNA reverse transcription, 2 ug of the isolated RNA was used. A master mix was prepared using the 2x reverse transcription master mix (Applied Biosystems, USA) and RNA was added. The reaction was started on the Biorad Thermal Cycler in Simport Amplitude PCR Reaction Stripes (ThermoFisher, USA). The reaction was run for 10 min at 25°C, for 2 hours at 37°C, for 5 minutes at 85°C and then stopped at 4°C.

### **2.3.3. qPCR**

To quantify mRNA levels of *Dpp3*, Glycerinaldehyd-3-phosphat-Dehydrogenase (GAPDH) was used. A primer-master mix was prepared with the GAPDH control mix (Applied Biosystems, USA), DPP3 primer (Applied Biosystems, USA) and TaqMan gene expression Master mix (Applied Biosystems, USA). The qPCR was performed in triplicates, which is why also a cDNA-master mix was prepared (2 ul of cDNA and 7 ul of dH<sub>2</sub>O). The reagents were pipetted into a Bio-Rad plate, and the qPCR was started on the Bio-Rad CFX Connect Real Time system (Bio-Rad, USA).

## **2.4. Protein isolation, SDS-Page and western blotting**

To gain whole protein lysates  $1 \times 10^6$  cells were seeded on 10 cm petri dish and subjected to hyperoxia treatment as previously described. After the treatment, cells were washed with 1x PBS, trypsinized and centrifuged at 1600 rpm for 4 minutes at 4°C. The resulting pellet was then resuspended in ~350 µL radioimmunoprecipitation assay buffer (RIPA, ThermoFisher, USA). The samples were vortexed for 1 minute, the cell lysates were centrifuged at 15000 rpm for 20 minutes at 4°C, and the protein concentration was measured with Pierce™ BCA Protein Assay Kit (Thermofisher, USA). The measurement of the samples, and the creation of the standardcurve for the calculation of protein concentrations was performed as described in the instructions of the kit.

Per lane, 20 µg of samples were separated by sodium dodecyl sulfate-polyacrylamide gel electrophoresis (SDS-PAGE). The gel consists of 10% separating gel (pH 8.8) and 4% stacking gel (pH 6.8). The electrophoresis is run at 100 V for 30 minutes and at 160 V for 1 hour.

PageRuler™ Prestained Protein Ladder (ThermoFisher Scientific, USA) was used for determination of protein size.

The separated proteins were transferred onto a nitrocellulose-membrane (VWR International, USA) under constant 250 mA for one hour and the membrane was then blocked with 5% milk in 1x TBST for 1 hour. Then the membrane was incubated with primary antibody (Table 3) overnight at 4°C and after washing the membrane was incubated with secondary alkaline phosphatase coupled antibody (Table 3) for 1 hour at RT. For detection, 1-Step™ NBT/BCIP substrate (ThermoFisher, USA) was used.

Table 1: Primary and secondary antibodies used for western blot.

Primary Antibodies	Species	Dilution	Company (Catalog#)
DPP3 polyclonal Antibody	Rabbit	1:1000	ThermoFisher #PA5-21709
SOD2 monoclonal Antibody	Rabbit	1:1000	Cell Sign. #13141
NQO1 polyclonal Antibody	Rabbit	1:1000	Sigma #SAB1410299
HO-1 monoclonal Antibody	Rabbit	1:1000	Cell Sign. #5853
β-Actin Antibody	Rabbit	1:1000	Cell Sign. #4967
HSP90 polyclonal Antibody	Rabbit	1:1000	Proteintech #13171-1-AP
Secondary Antibody	Species	Dilution	Company (Catalog#)
Anti-Rabbit IgG Alkaline Phosphatase	Goat	1:5000	Sigma #A3687

## 2.5. DPP3 activity assay

To measure DPP3 activity, Arg<sub>2</sub>-β-naphtylamide (Arg<sub>2</sub>-βNA) was used as a substrate to perform a soluble enzyme activity assay. For the assay 20 µg of proteins were pipetted into a white microtiter plate and 45 µM Arg<sub>2</sub>-βNA in Tris-HCl buffer (pH 8,2) was added. Immediately after adding the substrate, the fluorescence of the product β-naphtylamine was measured for 15 minutes (Excitation 332 nm, Emission 420 nm) with Fluorescence Microplate Reader (Molecular Devices, USA). To calculate the DPP3 Activity in the samples, two standard curves with 230 µl of different Arg<sub>2</sub>-β-naphtylamide concentrations (0-100 µM and 0-700 nM) and 5 µl 50 nM purified DPP3 were created.

## 2.6. Isolation of subcellular fractions

For the fractionation, 1×10<sup>6</sup> cells were seeded on a 10 cm petri dish. The cells were washed with 1x PBS, then ice-cold 1x PBS was added and the cells were scraped off with a rubber policeman. The cells were centrifuged at 13000 rpm for 5 minutes at 4°C and resuspended in 500 µl of buffer A. The cell-suspension was homogenized for 15 seconds at medium power and

kept on ice during the homogenization. After 10 minutes on ice, 25  $\mu$ l NP-40 was added and the suspension was vortexed for 5 seconds. The cell-suspension was then centrifuged at 5000 rpm for 5 minutes at 4°C. The supernatant was then transferred into a new Eppendorf tube and labeled as cytosolic fraction. To the remaining pellet, 50  $\mu$ l of buffer C were added and the pellet was gently mixed without resuspending. The suspension was then rocked on ice for 30 minutes and then centrifuged at 14000 rpm for 10 minutes at 4°C. The nuclear fraction was then transferred to a new Eppendorf tube and both fractions were stored at -20°C until use.

To separate subcellular fractions homemade buffers, cytoplasmic fraction buffer and nuclear fraction buffer, were used (Table 2).

Table 2: Buffers for isolation of subcellular fractions

Cytosolic fraction buffer (Buffer A)	Nuclear fraction buffer (Buffer C)
10 mM HEPES pH 7,9	20 mM HEPES pH 7,9
10 mM KCl	25% Glycerol
0,1 mM EDTA	0,4 M NaCl
	1 mM EDTA

## 2.7. Immunofluorescence

For immunofluorescence staining,  $5 \times 10^4$  cells were seeded on coverslips, incubated at 37°C and 5% CO<sub>2</sub> in humid atmosphere overnight, and then incubated in normal conditions or in the hyperoxia chamber for 48 hours. Cells were washed with 1x PBS, fixated with 4% paraformaldehyde for 10 minutes and permeabilized with ice cold 100% methanol for 6 minutes at -20°C. The coverslips were blocked with 5% goat serum and 5% BSA in 0,1% PBS-Triton-X. After blocking, the cells were incubated with primary antibody (anti-DPP3, anti-Nrf2) (Table 1) overnight at +4°C and after washing with 1x PBS, they were incubated with secondary antibody (anti-rabbit igG, coupled with AF488) for 1 hour at room temperature (RT) (Table 1). After washing with 1x PBS, the coverslips were mounted on microscope slides using vectashield with DAPI (4',6-Diamidin-2-phenylindol) (Vector Laboratories, USA) and analyzed with the IX73 inverted microscope (Olympus, Japan), using magnification of 40x. The images were taken by creating z-stacks of the cells and deconvolution was performed with constrained iterative algorithm (cellSens Dimension imaging software, Olympus, Japan). This process helps to avoid false positive signals, as the signal of both DAPI and fluorescein isothiocyanate (FITC) is recorded from the same plane and out-of-focus light that interferes

with the signal is removed (<https://www.olympus-lifescience.com/en/resources/white-papers/deconvolution/>).

Table 3: Primary and secondary antibodies used for immunofluorescence

Primary Antibodies	Species	Dilution	Company (Catalog#)
DPP3 Polyclonal Antibody	Rabbit	1:500	ThermoFisher #PA5-21709
Anti-NRF2 antibody produced in rabbit	Rabbit	1:500	Sigma #SAB4501984
Secondary Antibody	Species	Dilution	Company (Catalog#)
Goat anti-Rabbit IgG, Alexa Fluor 488	Goat	1:500	ThermoFisher #A-11008

## 2.8. Cell viability – MTT assay

For the 3- (4,5-dimethylthiazol-2-yl) -2,5-diphenyl tetrazolium bromide (MTT) assay,  $1 \times 10^4$  cells were seeded in a 96-well plate and incubated overnight at in an incubator at 37°C and 5% CO<sub>2</sub> in humid atmosphere, and the cells were treated with hyperoxia for 48 hours. After hyperoxia treatment, media was removed, and cells were incubated in 50 µl of 1x MTT (Abcam, USA) for 3 hours in the incubator at 37°C, 5% CO<sub>2</sub> in humid atmosphere. After incubation 150 µl dimethyl sulfoxide (DMSO) was added to each well, cells were resuspended, and the plate was placed on a shaker for 20 minutes at RT. The absorbance was measured at  $\lambda = 570$  nm on the CLARIOstar plate reader (BMG Labtech, Germany).

## 2.9. ROS production

For ROS production assay  $2.5 \times 10^5$  cells were seeded in a 6-well plate and treated for 48 hours with hyperoxia. After the treatment the media was removed, cells were washed with 1x PBS and incubated in dark at RT for 20 min with phenol red-free DMEM (ThermoFisher, USA) with 10% FBS and 25 µM 2',7'-dichlorodihydrofluorescein diacetate (H<sub>2</sub>DCF-DA) (Sigma Aldrich, USA), which was used as a substrate. After incubation the cells were trypsinized and resuspended in 1x PBS. The fluorescence (excitation 495 nm, emission 527 nm) was measured for 15 minutes with CLARIOstar (BMG LABTECH, Germany).

## 2.10. Quantitative peroxide assay (H<sub>2</sub>O<sub>2</sub> assay)

Pierce<sup>TM</sup> Quantitative Peroxide Assay Kit (ThermoFisher Scientific, USA), specifically the aqueous-compatible formulation of this kit, was used to measure hydrogen peroxide (H<sub>2</sub>O<sub>2</sub>) concentrations in cell lysates. To each well of a 96-well plate, 20 µg of total protein was added in triplicates, and per well 200 µl of working reagent was added. The samples were incubated

for 15 minutes at RT on a shaker and the absorbance was measured at  $\lambda = 595$  nm on the CLARIOstar plate reader (BMG Labtech, Germany). To determine the concentration of  $H_2O_2$ , a standard curve was created, using different dilutions of  $H_2O_2$  stock solution, ranging between 1 – 1000  $\mu$ M.

### **2.11. Determination of lipid peroxidation using TBARS (thiobarbituric acid reactive substances) assay**

To measure the lipid peroxidation, 50  $\mu$ g of protein samples were mixed with 175  $\mu$ l 0,67% 2-Thiobarbituric acid (TBA) and 175  $\mu$ l 20% Trichloroacetic acid (TCA) and filled up to 500  $\mu$ l with ddH<sub>2</sub>O. The samples are heated at 95°C for 20 minutes and then cooled for one minute in an ice-cold water bath. After centrifugation at 16000g for 2 minutes at RT, the supernatant is transferred to a 96-well plate and the absorbance is measured at  $\lambda = 532$  nm on the CLARIOstar plate reader (BMG Labtech, Germany).

### **2.12. AnnexinV and PI apoptosis assay**

For the apoptosis assay,  $2.5 \times 10^5$  cells were seeded in a 6-well plate and treated for 48 hours with hyperoxia. The cells were trypsinized and washed with 1x PBS two times before centrifugation at 1700 rpm for 5 min at 4°C. Cells were resuspended in 100  $\mu$ l 1x BB and transferred into FACS-tubes. To each tube, 2  $\mu$ l FITC and 3  $\mu$ l PI (BD Biosciences, USA) were added and the cells were incubated for 15 minutes in the dark. After adding 300  $\mu$ l 1x BB the cells were analyzed on the FACS Canto II flow cytometer. The content of non-apoptotic cells, (AnV<sup>neg</sup>/PI<sup>neg</sup>), early apoptotic cells (AnV<sup>pos</sup>/PI<sup>neg</sup>), late apoptotic cells (AnV<sup>pos</sup>/PI<sup>pos</sup>), and dead cells (AnV<sup>neg</sup>/PI<sup>pos</sup>) was measured in percent.

### **2.13. Programs and statistics**

Statistical analysis was performed with GraphPad Prism 8.0 (GraphPad Software, USA). Data is presented as mean  $\pm$  SD and groups were compared with student's ttest with a p value < 0.05 to be significant. Flow cytometry was analyzed with FlowJo Software (Treestar, USA) and images of fluorescence microscopy were analyzed with cellSens Dimension software (Olympus, Japan).



### 3. Results

#### 3.1. Characterization of DPP3 in MCF-7 and MDA-MB-231 cell lines

Studies show that the presence of DPP3 promotes survival of cells or mice under oxidative stress (Lu et al., 2017; Menale et al., 2019; Ren et al., 2021; Tong et al., 2021). We wanted to examine in MCF-7 and MDA-MB-231 cell line, if hyperoxia treatment influences the expression of *Dpp3* on both gene and protein level, and the DPP3 activity. To confirm the expression levels western blotting and qPCR method were used, for DPP3 activity a soluble activity assay was used, and the experiments were performed with treated cells (hyperoxia) and compared to control.

##### 3.1.1. *Dpp3* transcript levels after hyperoxia treatment

The mRNA levels of *Dpp3* were analyzed using qPCR and measurements were normalized to GAPDH, for each cell line separately. Results showed no significant difference in gene expression in MCF-7 cell line when comparing treated group to control (Figure 4). In contrast, significant increase of *Dpp3* transcript levels was shown in the MDA-MB-231 cells after hyperoxia treatment, compared to control group (Figure 4). Measurements were normalized to GAPDH for each cell line separately.

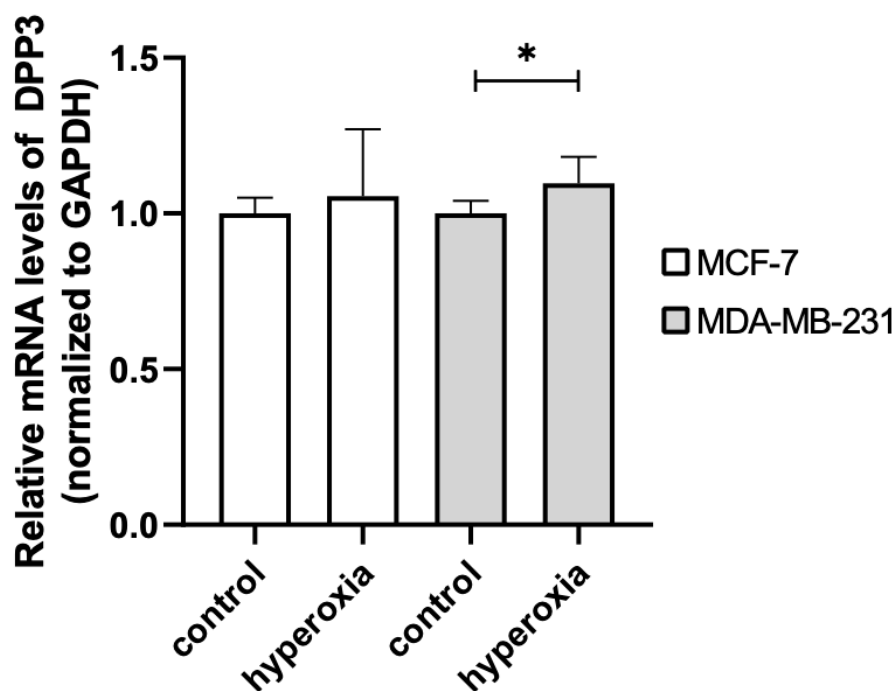


Figure 4: Analysis of mRNA levels of *Dpp3* using qPCR in MCF-7 and MDA-MB-231 cell lines. Cells were analyzed after hyperoxia treatment and compared to control group. The experiments were performed at least three times and representative data is presented. Results are presented as mean  $\pm$  SD. (Student's t-test: \* $p < 0.05$  control vs. hyperoxia MDA-MB-231)

### 3.1.2. *Dpp3* protein expression after hyperoxia treatment

To investigate if *Dpp3* protein expression is influenced by oxidative stress, we performed western blot. No change in *Dpp3* expression was observed in MCF-7 cells after hyperoxia treatment compared to control (Figure 5). Also, in MDA-MB-231 cell line, no change in DPP3 protein levels was found after hyperoxia treatment compared to control. What can be seen on the western blot (Figure 5) is that the MDA-MB-231 cell line has less DPP3 compared to the MCF-7 cell line. Next to DPP3, the housekeeping gene  $\beta$ -actin was detected for quantification.

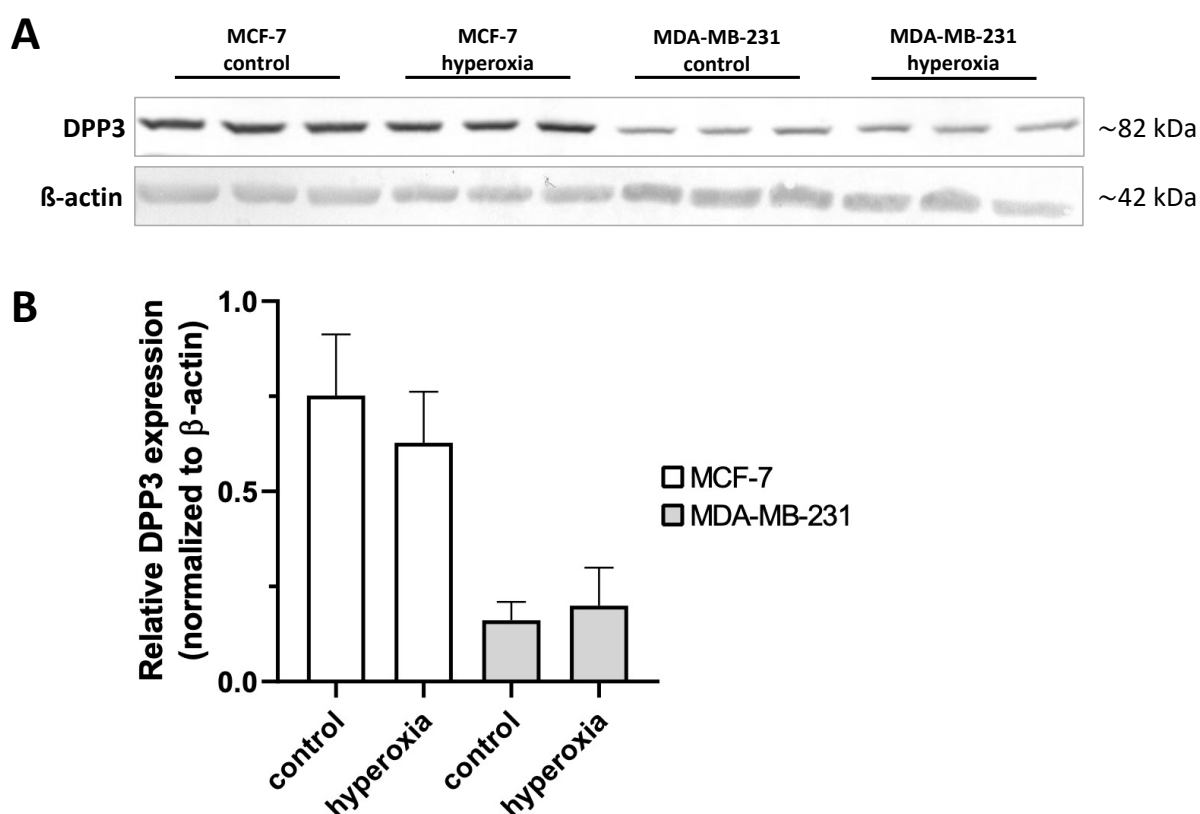


Figure 5: Analysis of *Dpp3* protein expression using western blot in MCF-7 and MDA-MB-231 cell lines. (A) Representative blot of *Dpp3* expression (B) Protein levels of DPP3 in MCF-7 and MDA-MB-231 cells in control and treated group (hyperoxia). The experiments were performed at least three times and representative data is presented. Results are presented as mean  $\pm$  SD. (Student's t-test: n.s.)

### 3.1.3. DPP3 activity after hyperoxia treatment

To complement the investigation of DPP3 mRNA and protein levels after hyperoxia treatment, the specific DPP3 activity was examined, using Arg2- $\beta$ -naphthylamide as a substrate. DPP3 activity was detected in control and hyperoxia treated group in both cell lines, although no significant change in enzymatic activity could be detected after hyperoxia treatment, when

results are compared to control group (Figure 6). There is no indication from these results that enzymatic activity of DPP3 is affected by the hyperoxia treatment.

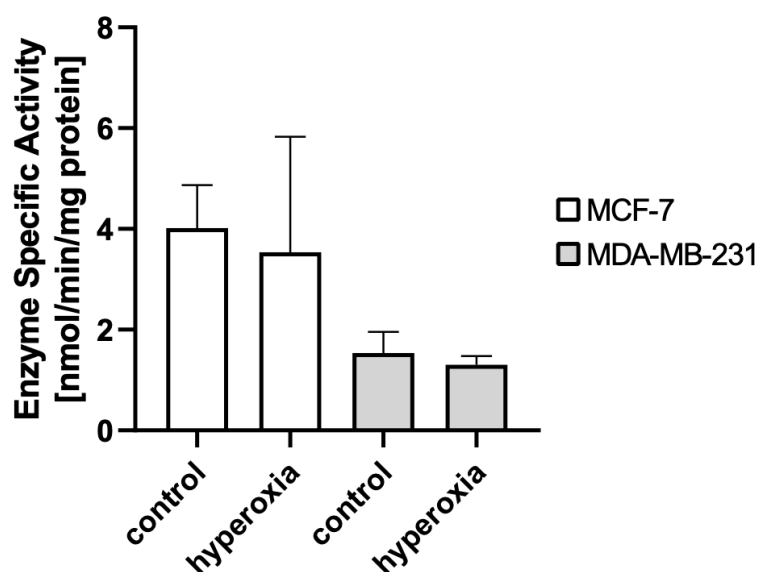


Figure 6: Enzyme specific activity of DPP3 in MCF-7 and MDA-MB-231 cell lines. Soluble DPP3 activity assay using Arg<sub>2</sub>-β-naphthylamide as a substrate was performed. The experiments were performed at least three times and representative data is presented. Results are presented as mean ± SD. (Student's t-test: n.s.)

### 3.2. Localization of DPP3 in MCF-7 and MDA-MB-231 cells

To investigate the localization of DPP3 and its dependency on oxidative stress, immunofluorescence was used, following western blot analysis of subcellular fractions. Additionally, DPP3 activity of subcellular fractions was analyzed.

#### 3.2.1. Immunofluorescence

Localization of DPP3 was analyzed with immunofluorescence using an Olympus IX73 inverted microscope (Olympus, USA). DPP3 signal was found in the cytosol and nucleus of both MCF-7 and MDA-MB-231 cells in both control and hyperoxia treated cells (Figure 7). There was no change in signal in either cell line after hyperoxia treatment compared to control in an extent that is visible to the unaided eye. The distribution of DPP3 seemed to be even throughout the cell, although in MCF-7 cells after hyperoxia treatment there are some more condensed signals of DPP3 in the nucleus. To prove that no unspecific antibody binding occurred, cells were additionally only incubated with secondary antibody (Figure S1). Nuclear permeabilization was tested by using anti-Nrf2 antibody, as Nrf2 is a known transcription factor in cells (Figure S2).

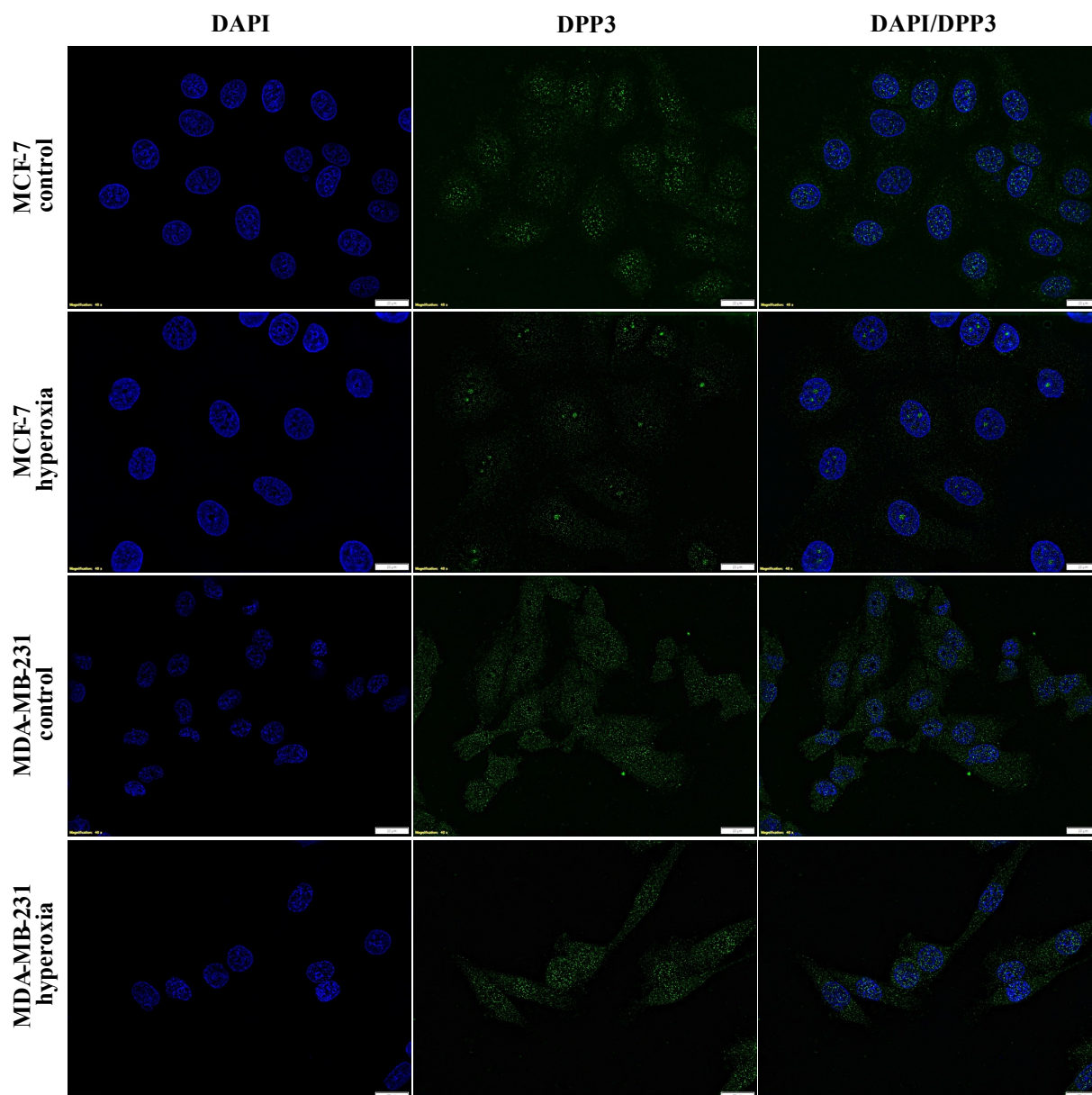


Figure 7: Immunofluorescence analysis of DPP3 in MCF-7 and MDA-MB-231 cell lines. DPP3 was detected using antibody conjugated with FITC (green) and nuclei were stained using DAPI (blue). The experiments were performed at least three times and representative data is presented.

### 3.2.2. *Dpp3* protein expression in cytosolic and nuclear fractions

Subcellular fractions (cytosolic and nuclear) were used to confirm localization of DPP3 in both cell lines using western blot. The western blot results showed slight impurity of the nuclear fractions in all examined groups, as HSP90 could be detected in almost all fractions (Figure 8). DPP3 was detected in the cytosol of all control and hyperoxia groups of both cell lines. DPP3 was also detected in nuclear fractions, although DPP3 seems to be present independently of hyperoxia treatment (Figure 8). The nuclear fraction was additionally analyzed with anti-HSP90 primary antibody to detect possible contaminations from cytosolic proteins in nuclear fraction.

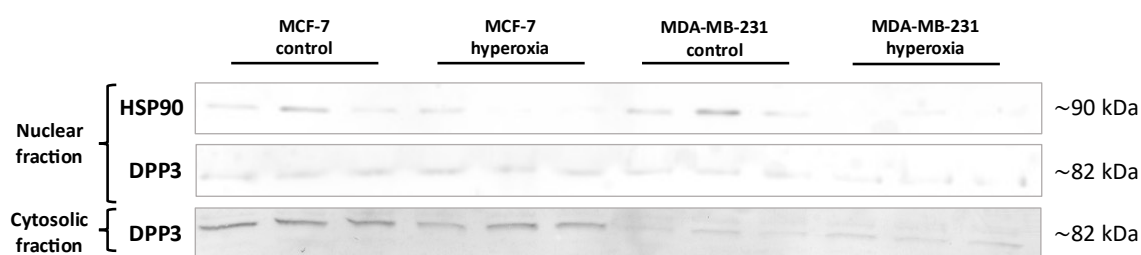


Figure 8: Expression of DPP3 in cytosolic and nuclear fractions of MCF-7 and MDA-MB-231 cell lines. DPP3 was detected in all treatment groups of both MCF-7 and MDA-MB-231 cell line. The experiments were performed at least three times and representative data is presented.

### 3.2.3. DPP3 activity assay in cytosolic and nuclear fractions

The enzymatic activity of DPP3 in cytosolic and nuclear fractions was determined with a soluble activity assay using Arg2- $\beta$ -naphthylamide as a substrate. Results of activity assay show fluorescence increase in both MCF-7 and MDA-MB-231 cell line in the cytosolic fraction over time, but not in the nuclear fraction. Enzyme specific activity of DPP3 was found in MCF-7 cell line (Figure 9A) and MDA-MB-231 cell line (Figure 9B) in the cytosolic fraction but is significantly decreased in the nuclear fraction. This activity seems to be independent of hyperoxia treatment, as results show no change in DPP3 activity in hyperoxia treatment group, compared to control.

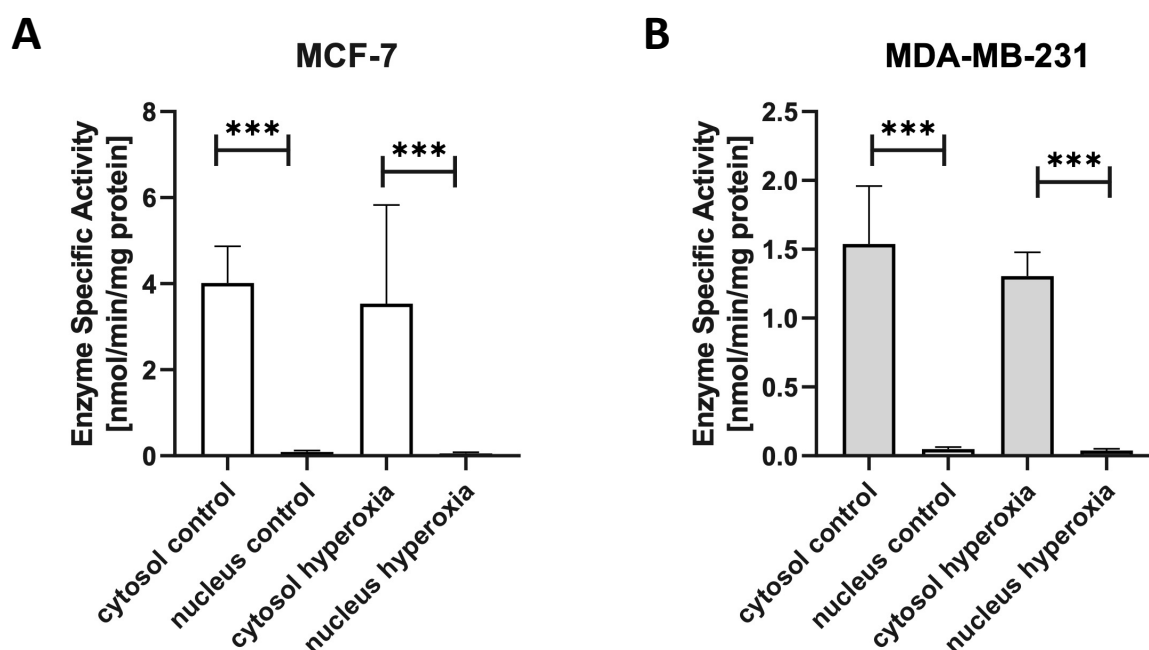


Figure 9: DPP3 activity in cytosolic and nuclear fractions of MCF-7 and MDA-MB-231 cell lines. (A) Enzyme specific activity in MCF-7 cells. (Student's t-test: \*\*\* $p$ <0.001, cytosolic fraction vs. nuclear fraction MCF-7) (B) Enzyme specific activity in MDA-MB-231 cells. (Student's t-test: \*\*\* $p$ <0.001, cytosolic fraction vs. nuclear fraction MDA-MB-231) The experiments were performed at least three times and representative data is presented. Results are presented as mean  $\pm$  SD.

### 3.3. Characterization of MCF-7 and MDA-MB-231 cell lines after hyperoxia treatment

The antioxidative response of MCF-7 and MDA-MB-231 cell lines was investigated after hyperoxia treatment. The availability of reducing agents, namely NAD(P)H was investigated with the MTT-assay. Furthermore, expression of the ARE proteins NQO1, HO-1 and SOD2 was checked with western blot. To check the production of ROS and the capacity of the cells to eliminate those ROS, total ROS production and H<sub>2</sub>O<sub>2</sub> concentration was measured. Furthermore, cell damage was analyzed by investigating lipid peroxidation with a TBARS assay, and cell viability or more specifically apoptosis was analyzed using AnnexinV/PI assay.

#### 3.3.1. Analyzing NAD(P)H availability with MTT assay

The tetrazolium salt MTT [3-(4,5-dimethylthiazol-2-yl)-2,5-diphenyl tetrazolium bromide] was used in a colorimetric assay for measurement of NAD(P)H availability. The results showed significantly reduced signal of blue formazan after the hyperoxia treatment compared to control in MCF-7 cell line (Figure 10). Also, in MDA-MB-231 cell line signal of formazan was reduced significantly after hyperoxia treatment compared to control (Figure 10).

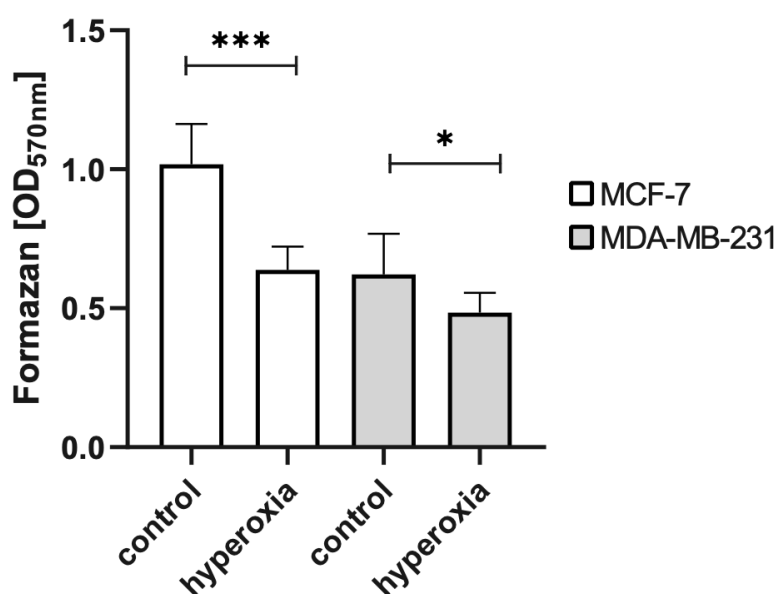


Figure 10: Analysis of NAD(P)H availability using MTT assay in MCF-7 and MDA-MB-231 cell lines. The experiments were performed at least three times and representative data is presented. Results are presented as mean  $\pm$  SD. (Student's t-test: \*\*\* $p$ <0.001, control vs. hyperoxia MCF-7, \* $p$ <0.05, control vs. hyperoxia MDA-MB-231)



### 3.3.2. Expression of ARE proteins after hyperoxia treatment

To determine the cellular response against oxidative stress, the expression of SOD2, NQO1 and HO-1 was analyzed through western blotting. SOD2, NQO1 and HO-1 were reliably detected in MCF-7 cell line in control and hyperoxia group but could not be detected in the MDA-MB-231 cell line (Figure 11A). These proteins seem to be expressed in the MDA-MB-231 cell line below the limit of detection with western blot. In MCF-7 cells, the level of NQO1 was significantly decreased in hyperoxia group compared to control (Figure 11B). In contrast, HO-1 levels in MCF-7 cells showed significant increase in hyperoxia group when compared to control (Figure 11C). However, SOD2 was detected in both cell lines in control and hyperoxia groups (Figure 11A). Even though it was detected, no significant change of SOD2 expression was observed in either cell line, when control is compared with hyperoxia group (Figure 11D). In addition to SOD2, NQO1 and HO-1,  $\beta$ -actin was detected for quantification of the signal.

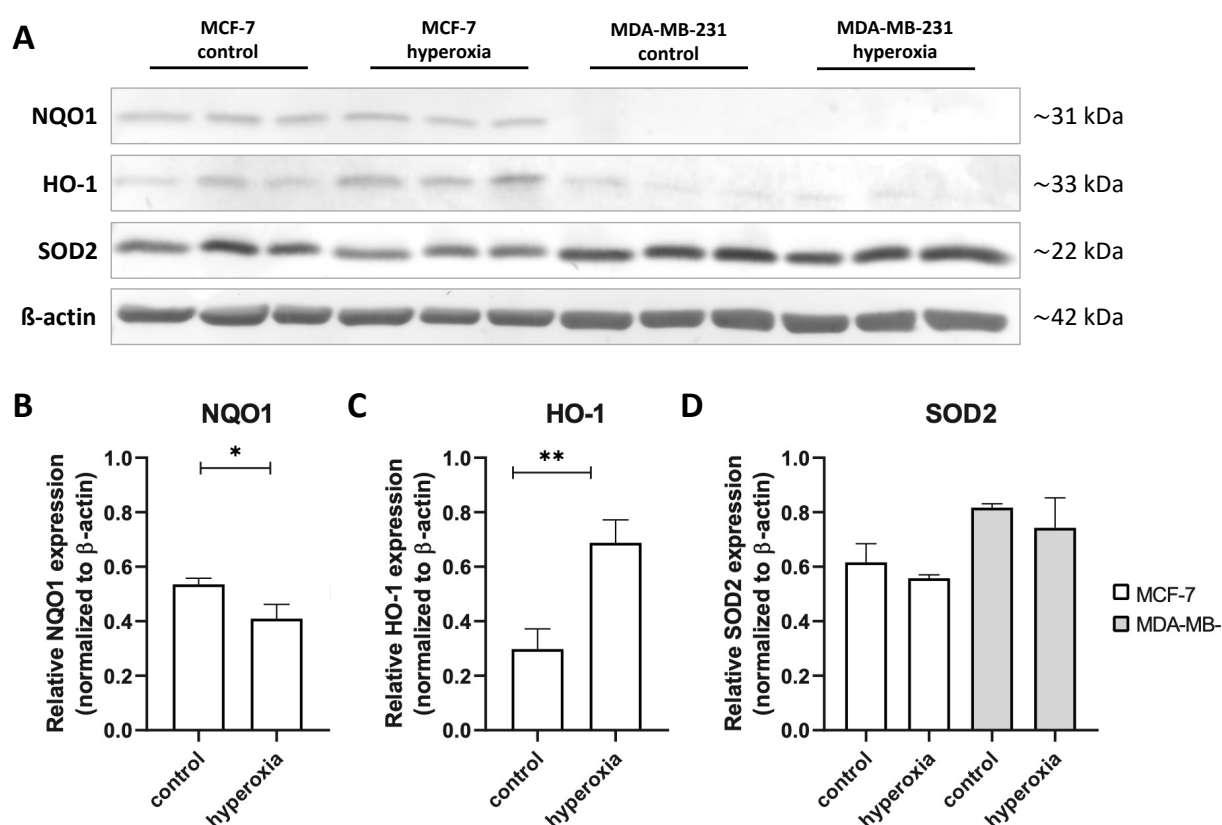


Figure 11: Protein expression of the ARE genes SOD2, NQO1 and HO-1 in MCF-7 and MDA-MB-231 cell lines. (A) Representative blots of NQO1, HO-1 and SOD2 and  $\beta$ -actin. MDA-MB-231 cells do not show expression of NQO1 or HO-1. (B) NQO1 expression in MCF-7 cell line (Student's t-test:  $*p < 0.05$ , control vs. hyperoxia). (C) HO-1 expression in MCF-7 cell line (control vs. hyperoxia;  $**p < 0.01$ , control vs. hyperoxia). (D) SOD2 expression in MCF-7 and MDA-MB-231 cell lines (Student's t-test: n.s.). The experiments were performed at least three times and representative data is presented. Results are presented as mean  $\pm$  SD.

### 3.3.1. Total ROS production after hyperoxia treatment

The total ROS production was measured using the substrate 2',7'-dichlorodihydrofluorescein diacetate (H<sub>2</sub>DCFDA). Content of total ROS in cells shows a tendency to decrease after the hyperoxia treatment compared to control group in both MCF-7 and MDA-MB-231 cell line (Figure 12). However, only in the MDA-MB-231 cell line this decrease of total ROS production after hyperoxia treatment compared to control is significant. The hyperoxia treatment did not cause an increase in reactive oxygen species.

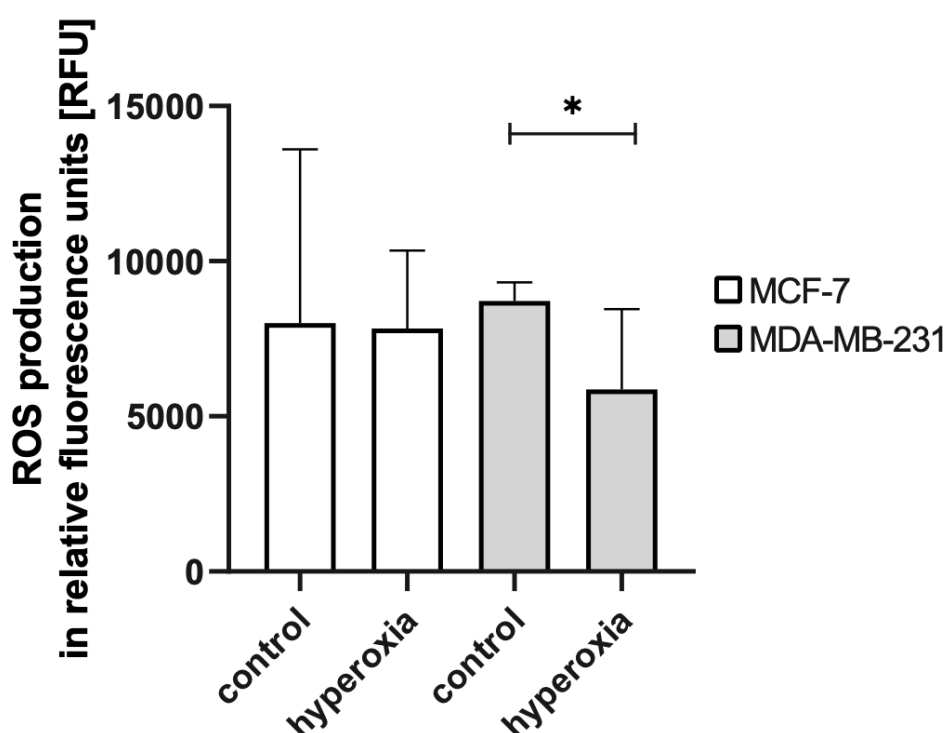


Figure 12: Total ROS production after hyperoxia treatment. The experiments were performed at least three times and representative data is presented. Results are presented as mean  $\pm$  SD. (Student's t-test: \* $p < 0.05$ , control vs. hyperoxia, MDA-MB-231)

### 3.3.1. Hydrogen peroxide concentration after hyperoxia treatment

In addition to measuring total ROS production, the concentration of H<sub>2</sub>O<sub>2</sub> in protein lysate was measured with the quantitative peroxide assay kit. The quantitative peroxide assay showed a significant decrease of H<sub>2</sub>O<sub>2</sub> in MCF-7 hyperoxia group, compared to control. In MDA-MB-231 hyperoxia group there is a trend to a decrease of H<sub>2</sub>O<sub>2</sub> if compared to control, although this difference is not significant (Figure 13). Hyperoxia treatment did not cause an increase in H<sub>2</sub>O<sub>2</sub> levels.



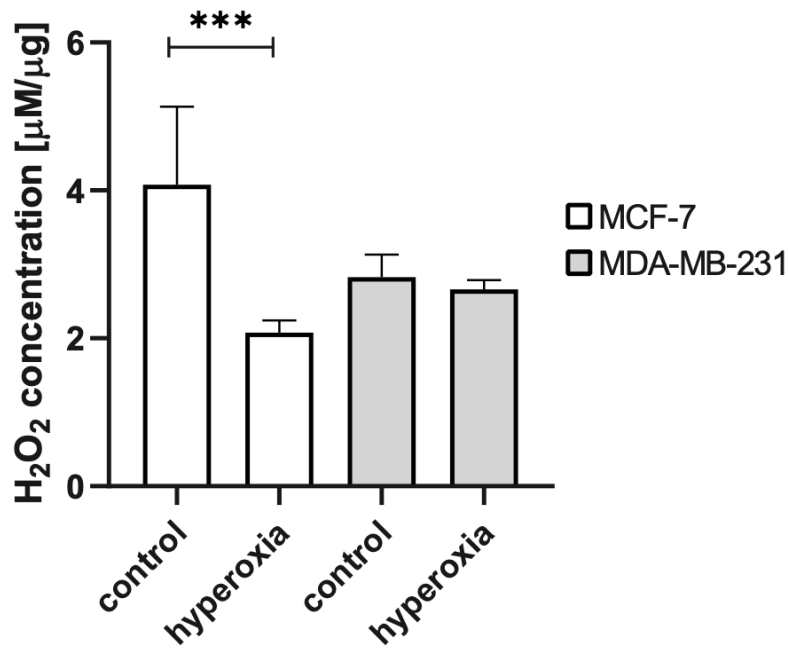


Figure 13: Hydrogen peroxide concentration after hyperoxia treatment. The experiments were performed at least three times and representative data is presented. Results are presented as mean  $\pm$  SD. (Student's t-test: \*\*\* $p < 0.001$ , control vs. hyperoxia MCF-7)

### 3.3.1. Lipid peroxidation after hyperoxia

Cell damage by lipid peroxidation was examined by measuring the amount of malondialdehyde (MDA) using a thiobarbituric acid reacting substances (TBARS) assay. Results show no change of malondialdehyde content after hyperoxia treatment compared to control in both MCF-7 and MDA-MB-231 cell line (Figure 14).

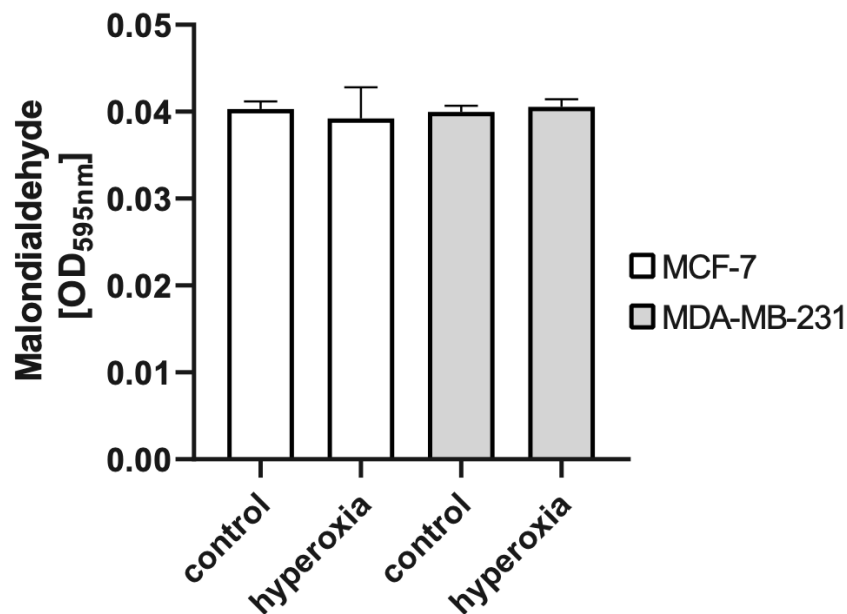


Figure 14: Analysis of lipid peroxidation by TBARS assay in MCF-7 and MDA-MB-231 cell lines. The experiments were performed at least three times and representative data is presented. Results are presented as mean  $\pm$  SD. (Student's t-test: n.s.)

### 3.3.1. Analysis of apoptosis with AnnexinV/PI assay

To investigate if the hyperoxia treatment has an impact on apoptosis in the MCF-7 and MDA-MB-231 cell lines, AnnexinV/PI apoptosis assay was performed. Gating was performed to remove debris from the analysis (Figure S3) and cells can be distinguished as double negative living cells, Annexin V positive early apoptotic cells, double positive late apoptotic cells, and PI positive dead cells (Figure S4). A significant increase of early apoptotic cells could be detected in the MCF-7 cell line in hyperoxia treatment group, compared to control (Figure 15B). Otherwise, there is no significant change of live cells (Figure 15A), apoptotic cells (Figure 15B and 15C) or dead cells (Figure 15D) in either MCF-7 and MDA-MB-231 cell lines if control is compared to hyperoxia treated cells.

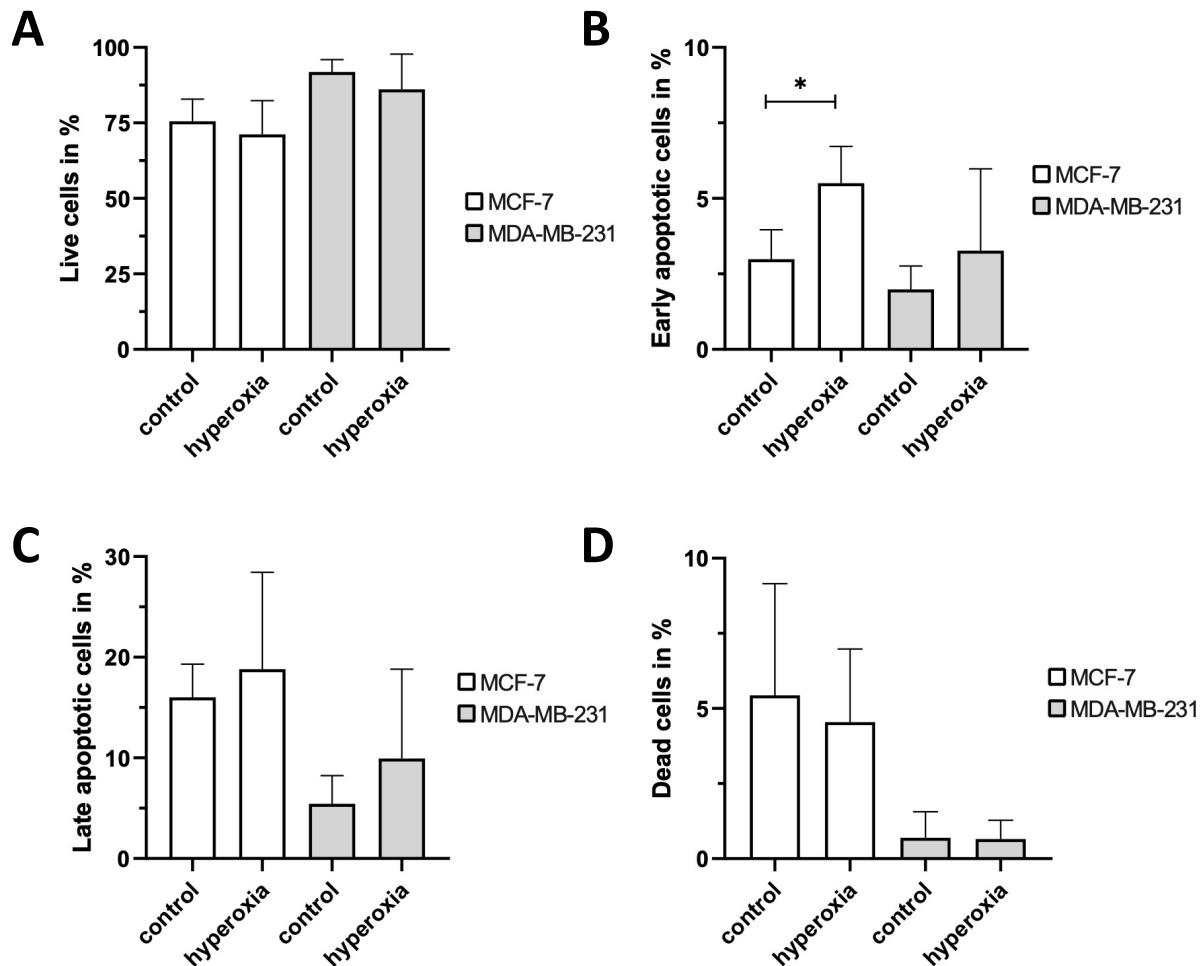


Figure 15: Analysis of apoptosis with AnnexinV/PI apoptosis assay in MCF-7 and MDA-MB-231 cell lines. (A) Live cells in percentage (Student's ttest: n.s.) (B) Early apoptotic cells in percentage (Student's ttest: \* $p < 0.05$  control vs. hyperoxia MCF-7) (C) Late apoptotic cells in percentage (Student's ttest: n.s.) (D) Dead cells in percentage (Student's ttest: n.s.) The experiments were performed at least three times and representative data is presented. Results are presented as mean  $\pm$  SD.

## 4. Discussion

Dipeptidyl peptidase 3 (DPP3) was found to be overexpressed in breast cancer (Lu et al., 2017) and therefore two breast cancer cell lines that express DPP3, namely MCF-7 and MDA-MB-231 were chosen for this research. As DPP3 is involved in the Keap1-Nrf2-ARE pathway (Lu et al., 2017), we wanted to see if treatment with hyperoxia effects DPP3 in breast cancer cells in terms of gene and protein expression and activity.

Levels of mRNA and protein are often used as biomarkers for diagnostics in cancer and other diseases (Cuzick et al., 2011; Xi et al., 2017). Quantitative PCR using hydrolysis probes can be used to determine gene expression levels by using a fluorescence quenching system (Singh & Roy-Chowdhuri, 2016). The determined increase in fluorescence is then quantified by normalizing the signal to a reference gene like GAPDH. qPCR was performed to determine the levels of *Dpp3* expression in breast cancer cells subjected to hyperoxia treatment. We found significant increase of transcript levels in the MDA-MB-231 cell line in hyperoxia treated cells compared to untreated cells (Figure 4). In the MCF-7 cell line no change in *Dpp3* transcript levels was found after hyperoxia treatment. So, although we could increase *Dpp3* levels in the MDA-MB-231 cell line by inducing oxidative stress, the same cannot be said for the MCF-7 cell line.

We performed western blot to determine the protein levels of DPP3 in the MCF-7 and MDA-MB-231 cell line subjected to hyperoxia treatment. Additionally, the DPP3 activity was analyzed with a soluble activity assay to determine change in DPP3 activity after hyperoxia treatment. During the activity assay the substrate Arg2- $\beta$ -naphthylamide is converted by DPP3 to  $\beta$ -naphthylamine, which is fluorescent and can therefore be measured with a fluorimeter. No significant change in protein expression (Figure 5) or DPP3 activity (Figure 6) that was caused by hyperoxia treatment was observed.

The question is, why only transcript levels of *Dpp3* in MDA-MB-231 cell line were affected. The regulation of gene expression is very complex, thereby the correlation between mRNA levels and protein levels is still not fully understood (Buccitelli & Selbach, 2020). In steady-state systems, mRNA levels mostly do correlate with protein levels (Liu et al., 2016). However, after inducing increase of mRNA abundance, there is a notable time shift before protein levels are elevated (Lee et al., 2011), which is caused by mRNA maturation, export, and translation (Buccitelli & Selbach, 2020; Liu et al., 2016). Therefore, a possible reason why we can observe change in mRNA levels but not protein levels is that the translation of mRNA is still ongoing when protein levels are analyzed. Moreover, *Dpp3* protein levels could be influenced by

translation rate or mRNA and protein degradation (Buccitelli & Selbach, 2020; Liu et al., 2016). In summary, we conclude that in MDA-MB-231 cell line *Dpp3* expression can be induced with hyperoxia treatment. We may gain better insight, if the sample size is increased, as biological systems have high variability on their own (Ilan, 2020).

In the literature, DPP3 is mostly described as a cytosolic protein (Grdiša & Vitale, 1991; Ohkubo et al., 2000), although DPP3 was also found in the nucleus in mice (Mačák Šafranko et al., 2015; Sobočanec et al., 2016). We investigated the localization of DPP3 by performing immunostaining on MCF-7 and MDA-MB-231 cells and by performing western blot and DPP3 activity assay on subcellular fractions. The cells were again treated with hyperoxia, to determine if DPP3 localization is influenced by oxidative stress. After comparing the results of western blot analysis, enzyme activity assay and immunofluorescence staining we conclude that DPP3 seems to be localized in the cytosol as well as the nucleus of the examined breast cancer cells. The results of the western blot from cytosolic and nuclear fractions show DPP3 in the nucleus as well as in the cytosol (Figure 8). Although it is possible that this signal is detected due to impurity of the nuclear fraction, the immunofluorescence, which is a much more sensitive method, also showed localization of DPP3 in the nucleus (Figure 7). However, the activity assay (Figure 9) showed no DPP3 activity in the nucleus, which leads us to believe that either DPP3 is inactive in the nucleus – for example as a result of change in protein formation or denaturation – or the inactivity can be explained due to the low concentrations of DPP3 in the nucleus. These results lead to the question how DPP3 might be able to enter the nucleus and why the protein is localized in the nucleus at all. As DPP3 does not have a NLS it needs another way of entering the nucleus (Fried & Kutay, 2003; Lu et al., 2021).

As mentioned before, due to its size of 82 kDa it seems unlikely that DPP3 enters the nucleus via diffusion, as the nuclear pores do not usually allow proteins of this size to enter this way (Cautain et al., 2015; Fried & Kutay, 2003). DPP3 might use an alternative mechanism to translocate into the nucleus, for instance the “piggyback” mechanism (Cautain et al., 2015), although this would need to be further examined. Interestingly, Keap1 has been described as a shuttling protein that migrates between nucleus and cytoplasm (Karapetian et al., 2005; Nguyen et al., 2005). This opens the question if DPP3 can be translocated into the nucleus in Keap1-DPP3 complex since we know that those proteins can form a complex. It has also been indicated that the Keap1-Nrf2 complex is translocated into the nucleus (Karapetian et al., 2005), and moreover it has been suggested that Keap1 might have a NLS (Karapetian et al., 2005), which

supports the possibility of DPP3 translocation via complex. Furthermore, DPP3 might have a nuclear localization signal that has not yet been identified.

Optimizing the experimental setup of the subcellular fractionation to avoid contaminations would be convenient and the western blotting should be repeated to get clearer information of the localization of DPP3. Another option for localization would be to label DPP3 with a fluorescent protein such as green fluorescent protein (Seibel et al., 2007) and perform fluorescent microscopy, which was done in human cells before (Feng et al., 2017).

Cancer cells experience more production of ROS because of their elevated metabolism. As a result of this, the antioxidant response system is often increased in cancer cells (Martínez-Reyes & Chandel, 2021). The response of the breast cancer cell lines to hyperoxia treatment was determined with multiple experiments.

The MTT assay is used widely as a measure of cell viability, proliferation, or metabolic activity (Lü et al., 2012; Stockert et al., 2012). However, the tetrazolium salt MTT is reduced by reducing agents in the cells to a measurable formazan (Stockert et al., 2012), which does not directly indicate cell viability, proliferation, or metabolic activity. MTT is mainly reduced in the cytoplasm by NADH and NADPH, after the salt has entered the cell through endocytosis, which indicates that the MTT assay depends on the availability of reductants like NADH and NADPH (Lü et al., 2012; Stockert et al., 2012). Therefore, we conclude, that this assay mostly gives information about the availability of reducing agents such as NADPH or glutathione (Stockert et al., 2012) in cells. We performed the MTT assay on breast cancer cells subjected to hyperoxia treatment to investigate the status of reducing agents in those cells. We found a significant decrease of formazan in hyperoxia treated cells compared to untreated cells in both cell lines (Figure 10). Therefore, there is less amount of reducing agents available in cells after hyperoxia treatment. A possible reason could be, that the cells need these reducing agents to decrease the amount of ROS in the cells. Antioxidants, also reducing agents, are needed for antioxidant enzymes (Tu et al., 2019) and NADPH is particularly needed for function of glutathione reductase and thioredoxin reductase, which both consume  $H_2O_2$  (Munro et al., 2016). A strong response against oxidative stress could therefore lead to the depletion of NADPH and other reducing agents. To confirm this theory, the concentration of NADPH could be directly measured for instance with a colorimetric assay and compared to results of the MTT assay.

In cancer, Nrf2 levels are often elevated under basal conditions, leading to an increased activity of the Keap1-Nrf2-ARE pathway (Harris & DeNicola, 2020). To further analyze the antioxidant response of breast cancer cells to the hyperoxia treatment, the expression of the ARE was investigated with western blot. Some of these antioxidant proteins are SOD2, NQO1 and HO-1 and they are regulated by the Keap1-Nrf2-ARE pathway (Tu et al., 2019). These enzymes can help reduce free radicals in cells like superoxide and H<sub>2</sub>O<sub>2</sub> (Tu et al., 2019) and are thus key players of the antioxidant response.

The results showed inconsistent expression of those proteins (Figure 11). The levels of SOD2 remained unaffected by the hyperoxia treatment in both cell lines. NQO1 and HO-1 are not expressed in the MDA-MB-231 cells or are expressed below limit of detection through western blotting. In the MCF-7 cells, levels of NQO1 are increased significantly, but levels of HO-1 were decreased significantly after hyperoxia treatment. HO-1 is converting heme to antioxidant bile pigments and CO and is a NADPH dependent protein (Dennery, 2014). NQO1 also relies on NAD(P)H, as it catalyzes antioxidant reductions (Dinkova-Kostova & Talalay, 2010). The expression of NQO1 and HO-1 is regulated by the Keap1-Nrf2-pathway (Tu et al., 2019), but there are factors beyond gene expression like protein stability that effect levels of NQO1 and HO-1. These contradictory results may be better understood if the gene expression of those proteins is investigated through qPCR. To better understand the regulation of the AREs during hyperoxia, it may be helpful to perform qPCR and western blotting with more proteins of the antioxidant response, including SOD2, NQO1 and HO-1, but also adding further proteins like glutathione reductase and thioredoxin reductase (Tu et al., 2019).

Next, we investigated the effect of hyperoxia on total ROS production and H<sub>2</sub>O<sub>2</sub> concentration. When cells experience oxidative stress, there is an imbalance between ROS production and antioxidant metabolism (Menale et al., 2019). In cancer cells, the antioxidant capacity seems to be increased compared to normal cells, increasing survival of those cancer cells (Harris & DeNicola, 2020). The total ROS production can be measured using the substrate 2',7'-dichlorodihydrofluorescein diacetate (H<sub>2</sub>DCFDA). In the presence of ROS, H<sub>2</sub>DCFDA is oxidized, which leads to it emitting fluorescence that can be measured with a fluorescence plate reader (Wu & Yotnda, 2011). We showed that total ROS production did not increase after hyperoxia treatment of breast cancer cells (Figure 12). In fact, in MDA-MB-231 cells we showed a significant decrease of levels of total ROS after hyperoxia treatment. The hyperoxia treatment seems to cause a decrease in reactive oxygen species.

Similar results could be achieved by examining the H<sub>2</sub>O<sub>2</sub> concentrations in the same conditions. Both cell lines showed no increase of H<sub>2</sub>O<sub>2</sub> after hyperoxia treatment (Figure 13), and in MCF-7 cells the H<sub>2</sub>O<sub>2</sub> concentration was significantly decreased after hyperoxia treatment. This leads us to believe, that both cell lines cope differently with the oxidative stress, as the distribution of ROS seems to differ. The different mechanism of reduction of free radicals in the cell lines is supported by the results of ARE protein levels, as we showed that MDA-MB-231 cells do not express NQO1 and HO-1. The results also indicate that the antioxidant response of MCF-7 and MDA-MB-231 cells is extremely active, as levels of total ROS and H<sub>2</sub>O<sub>2</sub> are slightly lower after hyperoxia treatment than before. This could be explained by the cells reacting excessively, namely overshooting, to the altered conditions of hyperoxia.

One of the cytotoxic effects oxidative stress can have on cells is lipid peroxidation, the oxidation of lipids caused by free radicals (Ayala et al., 2014). To check for cell damage, lipid peroxidation was investigated by measuring the amount of malondialdehyde (MDA) in the protein lysate of the cells. MDA can be measured with the thiobarbituric acid reacting substances (TBARS) assay, as MDA reacts with TBA and builds a fluorescent red adduct (Ayala et al., 2014).

The experiment showed no change in MDA content and thereby in lipid peroxidation after hyperoxia treatment compared to untreated group in either cell line (Figure 14). Therefore, we conclude that there was no extensive cell damage, although it may be beneficial to also investigate in potential DNA and protein damage, for instance checking if protein carbonylation takes place. Although the carbonylation of proteins leads to multiple different molecules depending on the affected residues, reliable protocols to measure protein carbonylation have been developed, like the 2,4-dinitrophenylhydrazine assay (Baraibar, 2013).

Apoptosis can be initiated by intrinsic and extrinsic factors and is described as the programmed mode of cell death (Demchenko, 2013). As oxidative stress can lead to apoptosis in cells (Menale et al., 2019; Ray et al., 2012; Ren et al., 2021), AnnexinV/PI assay was performed to investigate the effect of the hyperoxia treatment on apoptosis. Fluorescence labeled AnnexinV binds with the help of Ca<sup>2+</sup> to phosphatidylserine and is used to detect apoptotic cells (Demchenko, 2013; Telford, 2018). The apoptosis assay also relies on Propidium iodide (PI), which is a dye that binds to DNA and therefore can only emit fluorescence if the membrane is ruptured (Demchenko, 2013). The combined staining with Annexin V and PI gives information about the stages of apoptosis (Telford, 2018). We showed that apoptosis was increased after 48

hours of hyperoxia treatment in MCF-7 cells, and that MDA-MB-231 cells show a trend with no significance towards apoptosis after hyperoxia treatment as well (Figure 15). This leads us to believe, that the hyperoxia did not kill the breast cancer cells, but it might lead to cell death if cells are exposed to hyperoxia for more than 48 hours. It was indicated in studies (Menale et al., 2019; Ren et al., 2021), that DPP3 protects cell against apoptosis under conditions of stress, which is why it may be convenient to perform this experiment with *dpp3* knockout cells, to see if this protective effect of DPP3 is present in breast cancer cells as well.

Interestingly, if we look at the *Dpp3* transcript levels of both cell lines and at the ROS and apoptosis data we can see a correlation between an increase of *Dpp3* and a better response against oxidative stress and therefore survival of the cells. In MCF-7 cells we saw no change in *Dpp3* transcript levels after hyperoxia, and we also found no change in ROS levels, but we showed more apoptotic cells after hyperoxia. In MDA-MB-231 cells on the other hand there was significant increase in *Dpp3* transcript levels, and we found a decrease of ROS levels and no indications of apoptosis. This leads us to believe that in MDA-MB-231 cells DPP3 promotes the reduction of ROS and protects the cells from apoptosis. Therefore, higher levels of *Dpp3* correlate with better survival of the cells, which was reported in research before (Ren et al., 2021).

In summary, the MCF-7 and MDA-MB-231 cells showed high antioxidant response, as no cell damage was detected and total ROS and H<sub>2</sub>O<sub>2</sub> levels were not increased after hyperoxia treatment. A possible explanation might be that the antioxidant response is elevated in general in those cancer cells, or that the cells reacted very strongly to the stressor. We also report a correlation between increase in *Dpp3* and better survival of the breast cancer cells. How and if DPP3 is involved in this antioxidant stress response and how relevant this involvement is in cancer could be investigated with *dpp3* knockout cells. As multiple studies (Lu et al., 2017; Menale et al., 2019; Ren et al., 2021) showed involvement of DPP3 in oxidative stress, we believe that DPP3 might have a beneficial effect on cancer cells during oxidative stress. Moreover, the breast cancer cells seemed to cope well with the hyperoxia treatment, further making *Dpp3* knockout cells an interesting study object.



## 5. References

- Ayala, A., Muñoz, M. F., & Argüelles, S. (2014). Lipid Peroxidation: Production, Metabolism, and Signaling Mechanisms of Malondialdehyde and 4-Hydroxy-2-Nonenal. *Oxidative Medicine and Cellular Longevity*, 2014, 1–31. <https://doi.org/10.1155/2014/360438>
- Baral, P. K., Jajčanin-Jozić, N., Deller, S., Macheroux, P., Abramić, M., & Gruber, K. (2008). The first structure of dipeptidyl-peptidase III provides insight into the catalytic mechanism and mode of substrate binding. *Journal of Biological Chemistry*, 283(32), 22316–22324. <https://doi.org/10.1074/jbc.M803522200>
- Baraibar, M. A., Ladouce, R., & Friguet, B. (2013). Proteomic quantification and identification of carbonylated proteins upon oxidative stress and during cellular aging. *Journal of Proteomics*, 92, 63–70. <https://doi.org/10.1016/j.jprot.2013.05.008>
- Baršun, M., Jajčanin, N., Vukelić, B., Špoljarić, J., & Abramić, M. (2007). *Human dipeptidyl peptidase III acts as a post-proline-cleaving enzyme on endomorphins*. 388(3), 343–348. <https://doi.org/doi:10.1515/BC.2007.039>
- Buccitelli, C., & Selbach, M. (2020). mRNAs, proteins and the emerging principles of gene expression control. *Nature Reviews Genetics*, 21(10), 630–644. <https://doi.org/10.1038/s41576-020-0258-4>
- Cautain, B., Hill, R., de Pedro, N., & Link, W. (2015). Components and regulation of nuclear transport processes. *FEBS Journal*, 282(3), 445–462. <https://doi.org/10.1111/febs.13163>
- Cuzick, J., Swanson, G. P., Fisher, G., Brothman, A. R., Berney, D. M., Reid, J. E., Mesher, D., Speights, V., Stankiewicz, E., Foster, C. S., Møller, H., Scardino, P., Warren, J. D., Park, J., Younus, A., Flake, D. D., Wagner, S., Gutin, A., Lanchbury, J. S., & Stone, S. (2011). Prognostic value of an RNA expression signature derived from cell cycle proliferation genes in patients with prostate cancer: a retrospective study. *The Lancet Oncology*, 12(3), 245–255. [https://doi.org/10.1016/S1470-2045\(10\)70295-3](https://doi.org/10.1016/S1470-2045(10)70295-3)
- Day, B. J. (2019). The science of licking your wounds: Function of oxidants in the innate immune system. *Biochemical Pharmacology*, 163, 451–457. <https://doi.org/10.1016/j.bcp.2019.03.013>
- Demchenko, A. P. (2013). Beyond annexin V: fluorescence response of cellular membranes to apoptosis. *Cytotechnology*, 65(2), 157–172. <https://doi.org/10.1007/s10616-012-9481-y>
- Deniau, B., Rehfeld, L., Santos, K., Dienelt, A., Azibani, F., Sadoune, M., Kounde, P. R., Samuel, J. L., Tolpannen, H., Lassus, J., Harjola, V. P., Vodovar, N., Bergmann, A., Hartmann, O., Mebazaa, A., & Blet, A. (2019). Circulating dipeptidyl peptidase 3 is a myocardial depressant factor: dipeptidyl peptidase 3 inhibition rapidly and sustainably improves

haemodynamics. *European Journal of Heart Failure*, 22(2), 290–299. <https://doi.org/10.1002/ejhf.1601>

Dennerly, P. A. (2014). Signaling function of heme oxygenase proteins. *Antioxidants & Redox Signaling*, 20(11), 1743–1753. <https://doi.org/10.1089/ars.2013.5674>

Dewaele, M., Maes, H., & Agostinis, P. (2010). ROS-mediated mechanisms of autophagy stimulation and their relevance in cancer therapy. *Autophagy*, 6(7), 838–854. <https://doi.org/10.4161/auto.6.7.12113>

Dhar, S. K., & St. Clair, D. K. (2012). Manganese superoxide dismutase regulation and cancer. *Free Radical Biology and Medicine*, 52(11–12), 2209–2222. <https://doi.org/10.1016/j.freeradbiomed.2012.03.009>

Dinkova-Kostova, A. T., & Talalay, P. (2010). NAD(P)H:quinone acceptor oxidoreductase 1 (NQO1), a multifunctional antioxidant enzyme and exceptionally versatile cytoprotector. *Archives of Biochemistry and Biophysics*, 501(1), 116–123. <https://doi.org/10.1016/j.abb.2010.03.019>

Ellis, S., & Nuenke, J. M. (1967). Dipeptidyl Arylamidase III of the Pituitary. *Journal of Biological Chemistry*, 242(20), 4623–4629. [https://doi.org/10.1016/S0021-9258\(18\)99503-7](https://doi.org/10.1016/S0021-9258(18)99503-7)

Feng, S., Sekine, S., Pessino, V., Li, H., Leonetti, M. D., & Huang, B. (2017). Improved split fluorescent proteins for endogenous protein labeling. *Nature Communications*, 8(1), 370. <https://doi.org/10.1038/s41467-017-00494-8>

Fried, H., & Kutay, U. (2003). Nucleocytoplasmic transport: taking an inventory. *Cellular and Molecular Life Sciences : CMLS*, 60(8), 1659–1688. <https://doi.org/10.1007/s00018-003-3070-3>

Gorrini, C., Harris, I. S., & Mak, T. W. (2013). Modulation of oxidative stress as an anticancer strategy. *Nature Reviews Drug Discovery*, 12(12), 931–947. <https://doi.org/10.1038/nrd4002>

Grdiša, M., & Vitale, L. (1991). Types and localization of aminopeptidases in different human blood cells. *International Journal of Biochemistry*, 23(3), 339–345. [https://doi.org/https://doi.org/10.1016/0020-711X\(91\)90116-5](https://doi.org/https://doi.org/10.1016/0020-711X(91)90116-5)

Gupta, S. C., Hevia, D., Patchva, S., Park, B., Koh, W., & Aggarwal, B. B. (2012). Upsides and Downsides of Reactive Oxygen Species for Cancer: The Roles of Reactive Oxygen Species in Tumorigenesis, Prevention, and Therapy. *Antioxidants & Redox Signaling*, 16(11), 1295–1322. <https://doi.org/10.1089/ars.2011.4414>

Harris, I. S., & DeNicola, G. M. (2020). The Complex Interplay between Antioxidants and ROS in Cancer. *Trends in Cell Biology*, 30(6), 440–451. <https://doi.org/10.1016/j.tcb.2020.03.002>

- Hashimoto, J. I., Yamamoto, Y., Kurosawa, H., Nishimura, K., & Hazato, T. (2000). Identification of dipeptidyl peptidase III in human neutrophils. *Biochemical and Biophysical Research Communications*, 273(2), 393–397. <https://doi.org/10.1006/bbrc.2000.2827>
- Hast, B. E., Goldfarb, D., Mulvaney, K. M., Hast, M. A., Siesser, P. F., Yan, F., Hayes, D. N., & Major, M. B. (2013). *Molecular and Cellular Pathobiology Proteomic Analysis of Ubiquitin Ligase KEAP1 Reveals Associated Proteins That Inhibit NRF2 Ubiquitination*. <https://doi.org/10.1158/0008-5472.CAN-12-4400>
- Hurt, E. M., Thomas, S. B., Peng, B., & Farrar, W. L. (2007). Molecular consequences of SOD2 expression in epigenetically silenced pancreatic carcinoma cell lines. *British Journal of Cancer*, 97(8), 1116–1123. <https://doi.org/10.1038/sj.bjc.6604000>
- Ilan, Y. (2020). Order Through Disorder: The Characteristic Variability of Systems. *Frontiers in Cell and Developmental Biology*, 8. <https://doi.org/10.3389/fcell.2020.00186>
- Jha, S., Taschler, U., Domenig, O., Poglitsch, M., Bourgeois, B., Pollheimer, M., Pusch, L. M., Malovan, G., Frank, S., Madl, T., Gruber, K., Zimmermann, R., & Macheroux, P. (2020). Dipeptidyl peptidase 3 modulates the renin–Angiotensin system in mice. *Journal of Biological Chemistry*, 295(40), 13711–13723. <https://doi.org/10.1074/jbc.RA120.014183>
- Ju, H.-Q., Gocho, T., Aguilar, M., Wu, M., Zhuang, Z.-N., Fu, J., Yanaga, K., Huang, P., & Chiao, P. J. (2015). Mechanisms of Overcoming Intrinsic Resistance to Gemcitabine in Pancreatic Ductal Adenocarcinoma through the Redox Modulation. *Molecular Cancer Therapeutics*, 14(3), 788–798. <https://doi.org/10.1158/1535-7163.MCT-14-0420>
- Karapetian, R. N., Evstafieva, A. G., Abaeva, I. S., Chichkova, N. v., Filonov, G. S., Rubtsov, Y. P., Sukhacheva, E. A., Melnikov, S. v., Schneider, U., Wanker, E. E., & Vartapetian, A. B. (2005). Nuclear Oncoprotein Prothymosin  $\alpha$  Is a Partner of Keap1: Implications for Expression of Oxidative Stress-Protecting Genes. *Molecular and Cellular Biology*, 25(3), 1089–1099. <https://doi.org/10.1128/MCB.25.3.1089-1099.2005>
- Kaufmann, P., Muenzner, M., Kästorf, M., Santos, K., Hartmann, T., Dienelt, A., Rehfeld, L., & Bergmann, A. (2019). A novel and highly efficient purification procedure for native human dipeptidyl peptidase 3 from human blood cell lysate. *PloS One*, 14(8), e0220866–e0220866. <https://doi.org/10.1371/journal.pone.0220866>
- Kim, Y. S., Gupta Vallur, P., Phaëton, R., Mythreye, K., & Hempel, N. (2017). Insights into the Dichotomous Regulation of SOD2 in Cancer. *Antioxidants (Basel, Switzerland)*, 6(4). <https://doi.org/10.3390/antiox6040086>
- Kumar, P., Reithofer, V., Reisinger, M., Wallner, S., Pavkov-Keller, T., Macheroux, P., & Gruber, K. (2016). Substrate complexes of human dipeptidyl peptidase III reveal the mechanism of enzyme inhibition. *Scientific Reports*, 6(1), 23787. <https://doi.org/10.1038/srep23787>

- Lee, M. V., Topper, S. E., Hubler, S. L., Hose, J., Wenger, C. D., Coon, J. J., & Gasch, A. P. (2011). A dynamic model of proteome changes reveals new roles for transcript alteration in yeast. *Molecular Systems Biology*, 7(1), 514. <https://doi.org/10.1038/msb.2011.48>
- Lee, S., & Hu, L. (2020). Nrf2 activation through the inhibition of Keap1–Nrf2 protein–protein interaction. *Medicinal Chemistry Research*, 29(5), 846–867. <https://doi.org/10.1007/s00044-020-02539-y>
- Liu, Y., Beyer, A., & Aebersold, R. (2016). On the Dependency of Cellular Protein Levels on mRNA Abundance. *Cell*, 165(3), 535–550. <https://doi.org/10.1016/j.cell.2016.03.014>
- Liu, Y., Kern, J. T., Walker, J. R., Johnson, J. A., Schultz, P. G., & Luesch, H. (2007). A genomic screen for activators of the antioxidant response element. *Proceedings of the National Academy of Sciences of the United States of America*, 104(12), 5205–5210. <https://doi.org/10.1073/pnas.0700898104>
- Lu, J., Wu, T., Zhang, B., Liu, S., Song, W., Qiao, J., & Ruan, H. (2021). Types of nuclear localization signals and mechanisms of protein import into the nucleus. *Cell Communication and Signaling*, 19(1), 60. <https://doi.org/10.1186/s12964-021-00741-y>
- Lu, K., Alcivar, A. L., Ma, J., Foo, T. K., Zywea, S., Mahdi, A., Huo, Y., Kensler, T. W., Gatz, M. L., & Xia, B. (2017). NRF2 induction supporting breast cancer cell survival is enabled by oxidative stress-induced DPP3-KEAP1 interaction. *Cancer Research*, 77(11), 2881–2892. <https://doi.org/10.1158/0008-5472.CAN-16-2204>
- Lü, L., Zhang, L., Wai, M. S. M., Yew, D. T. W., & Xu, J. (2012). Exocytosis of MTT formazan could exacerbate cell injury. *Toxicology in Vitro*, 26(4), 636–644. <https://doi.org/10.1016/j.tiv.2012.02.006>
- Mačak Šafranko, Ž., Sobočanec, S., Šarić, A., Jajčanin-Jozić, N., Krsnik, Ž., Aralica, G., Balog, T., & Abramić, M. (2015). The effect of 17 $\beta$ -estradiol on the expression of dipeptidyl peptidase III and heme oxygenase 1 in liver of CBA/H mice. *Journal of Endocrinological Investigation*, 38(4), 471–479. <https://doi.org/10.1007/s40618-014-0217-z>
- Martínez-Reyes, I., & Chandel, N. S. (2021). Cancer metabolism: looking forward. *Nature Reviews Cancer*, 21(10), 669–680. <https://doi.org/10.1038/s41568-021-00378-6>
- Mazzocco, C., Gillibert-Duplantier, J., Neaud, V., Fukasawa, K. M., Claverol, S., Bonneau, M., & Puiroux, J. (2006). Identification and characterization of two dipeptidyl-peptidase III isoforms in *Drosophila melanogaster*. *FEBS Journal*, 273(5), 1056–1064. <https://doi.org/10.1111/j.1742-4658.2006.05132.x>

- Menale, C., Robinson, L. J., Palagano, E., Rigoni, R., Erreni, M., Almarza, A. J., Strina, D., Mantero, S., Lizier, M., Forlino, A., Besio, R., Monari, M., Vezzoni, P., Cassani, B., Blair, H. C., Villa, A., & Sobacchi, C. (2019). Absence of Dipeptidyl Peptidase 3 Increases Oxidative Stress and Causes Bone Loss. *Journal of Bone and Mineral Research*, 34(11), 2133–2148. <https://doi.org/10.1002/jbmr.3829>
- Munro, D., Banh, S., Sotiri, E., Tamanna, N., & Treberg, J. R. (2016). The thioredoxin and glutathione-dependent H<sub>2</sub>O<sub>2</sub> consumption pathways in muscle mitochondria: Involvement in H<sub>2</sub>O<sub>2</sub> metabolism and consequence to H<sub>2</sub>O<sub>2</sub> efflux assays. *Free Radical Biology and Medicine*, 96, 334–346. <https://doi.org/10.1016/j.freeradbiomed.2016.04.014>
- Nguyen, T., Sherratt, P. J., Nioi, P., Yang, C. S., & Pickett, C. B. (2005). Nrf2 Controls Constitutive and Inducible Expression of ARE-driven Genes through a Dynamic Pathway Involving Nucleocytoplasmic Shuttling by Keap1. *Journal of Biological Chemistry*, 280(37), 32485–32492. <https://doi.org/10.1074/jbc.M503074200>
- Ohkubo, I., Li, Y. H., Maeda, T., Yamamoto, Y., Yamane, T., Du, P. G., & Nishi, K. (2000). Molecular cloning and immunohistochemical localization of rat dipeptidyl peptidase III. *Forensic Science International*, 113(1–3), 147–151. [https://doi.org/10.1016/S0739-0738\(00\)00200-0](https://doi.org/10.1016/S0739-0738(00)00200-0)
- Pang, X., Shimizu, A., Kurita, S., Zankov, D. P., Takeuchi, K., Yasuda-Yamahara, M., Kume, S., Ishida, T., & Ogita, H. (2016). Novel Therapeutic Role for Dipeptidyl Peptidase III in the Treatment of Hypertension. *Hypertension*, 68(3), 630–641. <https://doi.org/10.1161/HYPERTENSIONAHA.116.07357>
- Portakal, O., Özkaya, Ö., Erden inal, M., Bozan, B., Koşan, M., & Sayek, I. (2000). Coenzyme Q10 concentrations and antioxidant status in tissues of breast cancer patients. *Clinical Biochemistry*, 33(4), 279–284. [https://doi.org/10.1016/S0009-9120\(00\)00067-9](https://doi.org/10.1016/S0009-9120(00)00067-9)
- Prajapati, S. C., & Chauhan, S. S. (2011). Dipeptidyl peptidase III: A multifaceted oligopeptide N-end cutter. *FEBS Journal*, 278(18), 3256–3276. <https://doi.org/10.1111/j.1742-4658.2011.08275.x>
- Raghunath, A., Sundarraj, K., Nagarajan, R., Arfuso, F., Bian, J., Kumar, A. P., Sethi, G., & Perumal, E. (2018). Antioxidant response elements: Discovery, classes, regulation and potential applications. *Redox Biology*, 17, 297–314. <https://doi.org/10.1016/J.REDOX.2018.05.002>
- Ray, P. D., Huang, B.-W., & Tsuji, Y. (2012). Reactive oxygen species (ROS) homeostasis and redox regulation in cellular signaling. *Cellular Signalling*, 24(5), 981–990. <https://doi.org/10.1016/j.cellsig.2012.01.008>

- Rehfeld, L., Funk, E., Jha, S., Macheroux, P., Melander, O., & Bergmann, A. (2019). Novel Methods for the Quantification of Dipeptidyl Peptidase 3 (DPP3) Concentration and Activity in Human Blood Samples. *The Journal of Applied Laboratory Medicine*, 3(6), 943–953. <https://doi.org/10.1373/JALM.2018.027995>
- Ren, X., Yu, J., Guo, L., & Ma, H. (2021). Dipeptidyl-peptidase 3 protects oxygen-glucose deprivation/reoxygenation-injured hippocampal neurons by suppressing apoptosis, oxidative stress and inflammation via modulation of Keap1/Nrf2 signaling. *International Immunopharmacology*, 96. <https://doi.org/10.1016/j.intimp.2021.107595>
- Saeidnia, S., & Abdollahi, M. (2013). Antioxidants: Friends or foe in prevention or treatment of cancer: The debate of the century. *Toxicology and Applied Pharmacology*, 271(1), 49–63. <https://doi.org/10.1016/j.taap.2013.05.004>
- Sayin, V. I., Ibrahim, M. X., Larsson, E., Nilsson, J. A., Lindahl, P., & Bergo, M. O. (2014). Antioxidants Accelerate Lung Cancer Progression in Mice. *Science Translational Medicine*, 6(221). <https://doi.org/10.1126/scitranslmed.3007653>
- Seibel, N. M., Eljouni, J., Nalaskowski, M. M., & Hampe, W. (2007). Nuclear localization of enhanced green fluorescent protein homomultimers. *Analytical Biochemistry*, 368(1), 95–99. <https://doi.org/10.1016/j.ab.2007.05.025>
- Šimaga, Š., Babić, D., Osmak, M., Šprem, M., & Abramić, M. (2003). Tumor cytosol dipeptidyl peptidase III activity is increased with histological aggressiveness of ovarian primary carcinomas. *Gynecologic Oncology*, 91(1), 194–200. [https://doi.org/10.1016/S0090-8258\(03\)00462-1](https://doi.org/10.1016/S0090-8258(03)00462-1)
- Singh, C., & Roy-Chowdhuri, S. (2016). *Quantitative Real-Time PCR: Recent Advances* (pp. 161–176). [https://doi.org/10.1007/978-1-4939-3360-0\\_15](https://doi.org/10.1007/978-1-4939-3360-0_15)
- Sobočanec, S., Filić, V., & Matovina, M. (2016). Prominent role of exopeptidase DPP III in estrogen-mediated protection against hyperoxia in vivo. *Redox Biology*.
- Srinivas, U. S., Tan, B. W. Q., Vellayappan, B. A., & Jeyasekharan, A. D. (2019). ROS and the DNA damage response in cancer. *Redox Biology*, 25, 101084. <https://doi.org/10.1016/j.redox.2018.101084>
- Stockert, J. C., Blázquez-Castro, A., Cañete, M., Horobin, R. W., & Villanueva, Á. (2012). MTT assay for cell viability: Intracellular localization of the formazan product is in lipid droplets. *Acta Histochemica*, 114(8), 785–796. <https://doi.org/https://doi.org/10.1016/j.acthis.2012.01.006>
- Taguchi, K., & Yamamoto, M. (2017). The KEAP1-NRF2 System in Cancer. *Frontiers in Oncology*, 7, 85. <https://doi.org/10.3389/fonc.2017.00085>



Takagi, K., Blet, A., Levy, B., Deniau, B., Azibani, F., Feliot, E., Bergmann, A., Santos, K., Hartmann, O., Gayat, E., Mebazaa, A., & Kimmoun, A. (2019). Circulating dipeptidyl peptidase 3 and alteration in haemodynamics in cardiogenic shock: results from the OptimaCC trial. *European Journal of Heart Failure*, 22(2), 279–286. <https://doi.org/10.1002/ejhf.1600>

Telford, W. G. (2018). *Multiparametric Analysis of Apoptosis by Flow Cytometry* (pp. 167–202). [https://doi.org/10.1007/978-1-4939-7346-0\\_10](https://doi.org/10.1007/978-1-4939-7346-0_10)

Thannickal, V. J., & Fanburg, B. L. (2000). Reactive oxygen species in cell signaling. In *American Journal of Physiology - Lung Cellular and Molecular Physiology* (Vol. 279, Issues 6 23-6, pp. 1005–1028). American Physiological Society. <https://doi.org/10.1152/ajplung.2000.279.6.11005>

Tong, L., Chuang, C.-C., Wu, S., & Zuo, L. (2015). Reactive oxygen species in redox cancer therapy. *Cancer Letters*, 367(1), 18–25. <https://doi.org/10.1016/j.canlet.2015.07.008>

Tong, Y., Huang, Y., Zhang, Y., Zeng, X., Yan, M., Xia, Z., & Lai, D. (2021). DPP3/CDK1 contributes to the progression of colorectal cancer through regulating cell proliferation, cell apoptosis, and cell migration. *Cell Death & Disease*, 12(6), 529. <https://doi.org/10.1038/s41419-021-03796-4>

Tu, W., Wang, H., Li, S., Liu, Q., & Sha, H. (2019). The Anti-Inflammatory and Anti-Oxidant Mechanisms of the Keap1/Nrf2/ARE Signaling Pathway in Chronic Diseases. *Aging and Disease*, 10(3), 637–651. <https://doi.org/10.14336/AD.2018.0513>

Vasan, K., Werner, M., & Chandel, N. S. (2020). Mitochondrial Metabolism as a Target for Cancer Therapy. *Cell Metabolism*, 32(3), 341–352. <https://doi.org/10.1016/j.cmet.2020.06.019>

Wagner, P., Kunz, J., Koller, A., & Hall, M. N. (1990). Active transport of proteins into the nucleus. *FEBS Letters*, 275(1–2), 1–5. [https://doi.org/10.1016/0014-5793\(90\)81425-N](https://doi.org/10.1016/0014-5793(90)81425-N)

Wagstaff, K. M., & Jans, D. A. (2009). Importins and Beyond: Non-Conventional Nuclear Transport Mechanisms. *Traffic*, 10(9), 1188–1198. <https://doi.org/10.1111/j.1600-0854.2009.00937.x>

Warburg, O. (1956). On the Origin of Cancer Cells. *Science*, 123(3191), 309–314. <https://doi.org/10.1126/science.123.3191.309>

Weinberg, F., Hamanaka, R., Wheaton, W. W., Weinberg, S., Joseph, J., Lopez, M., Kalyanaraman, B., Mutlu, G. M., Budinger, G. R. S., & Chandel, N. S. (2010). Mitochondrial metabolism and ROS generation are essential for Kras-mediated tumorigenicity. *Proceedings of the National Academy of Sciences of the United States of America*, 107(19), 8788–8793. <https://doi.org/10.1073/pnas.1003428107>

Wu, D., & Yotnda, P. (2011). Production and Detection of Reactive Oxygen Species (ROS) in Cancers. *Journal of Visualized Experiments*, 57. <https://doi.org/10.3791/3357>

Xi, X., Li, T., Huang, Y., Sun, J., Zhu, Y., Yang, Y., & Lu, Z. (2017). RNA Biomarkers: Frontier of Precision Medicine for Cancer. *Non-Coding RNA*, 3(1), 9. <https://doi.org/10.3390/ncrna3010009>

Zhang, J., Wang, X., Vikash, V., Ye, Q., Wu, D., Liu, Y., & Dong, W. (2016). ROS and ROS-Mediated Cellular Signaling. *Oxidative Medicine and Cellular Longevity*, 2016, 1–18. <https://doi.org/10.1155/2016/4350965>

Websites:

<https://www.olympus-lifescience.com/en/resources/white-papers/deconvolution/> (11.01.2022)



## 6. Supplementary data

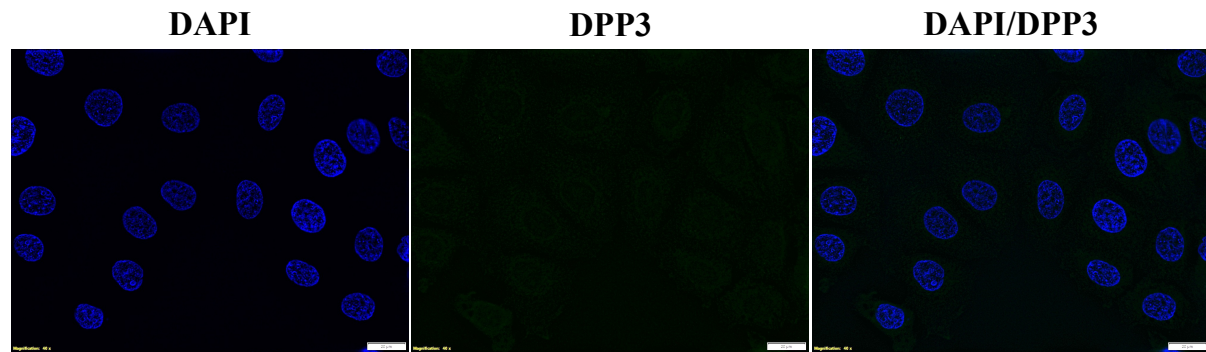


Figure S1: Representative negative control of immunofluorescence experiment. Cells were only incubated with secondary goat anti-rabbit AF488 conjugated antibody to check for unspecific antibody binding.

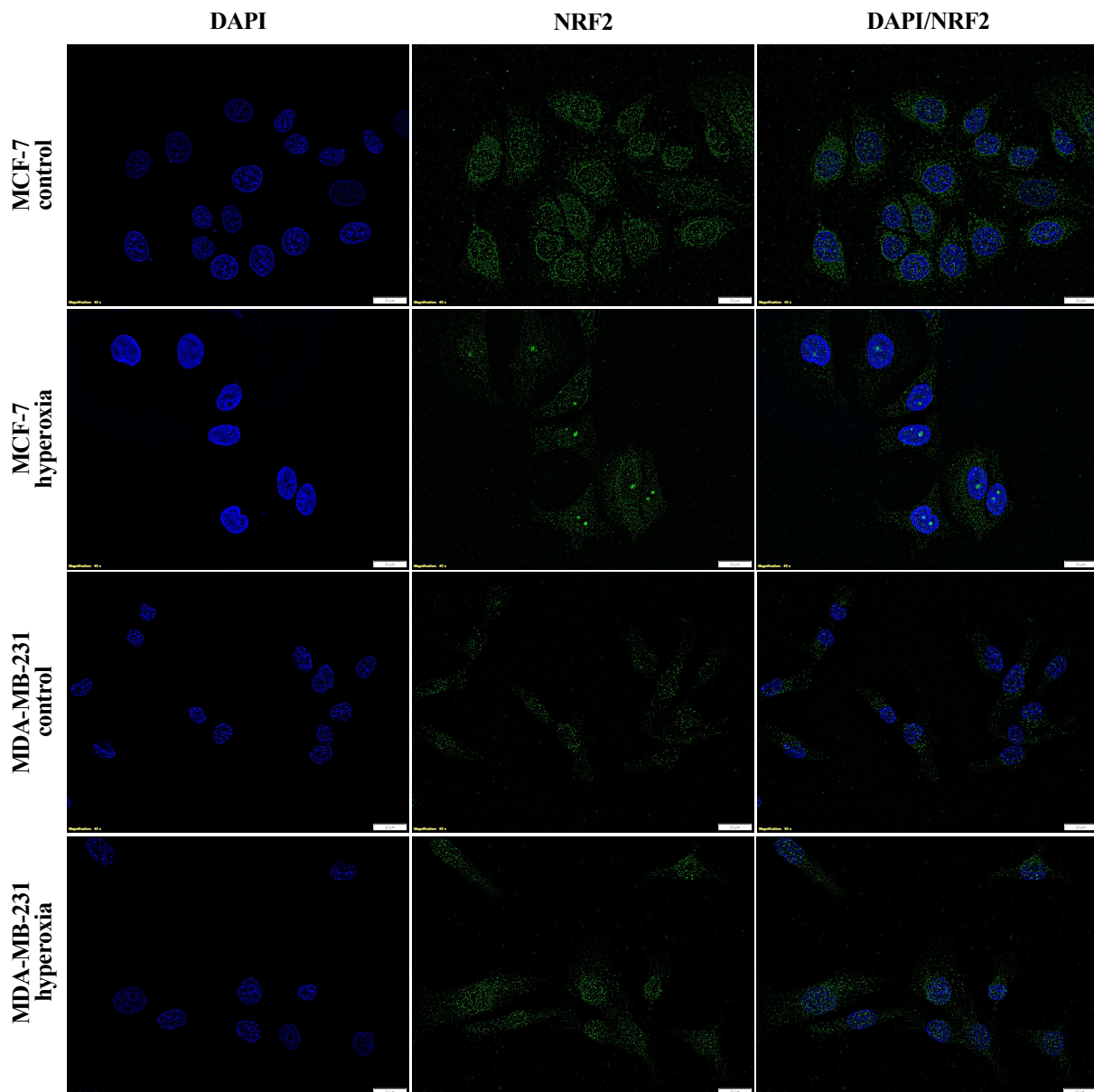


Figure S2: Immunofluorescence analysis of Nrf2 in MCF-7 and MDA-MB-231 cell lines. Nuclear permeabilization was tested with Nrf2-antibody. Nrf2 was detected using secondary antibody conjugated with FITC (green) and nuclei were stained using DAPI (blue). The experiments were performed at least three times and representative data is presented.

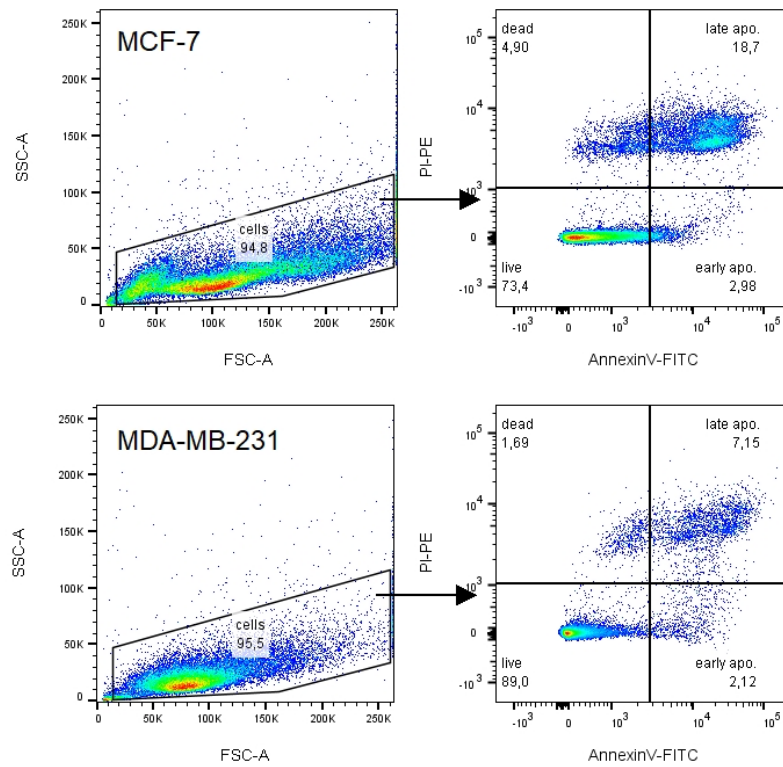


Figure S3: Plot of forward scatter versus side scatter of AnnexinV/PI data. Gating was performed to analyze AnnexinV/PI data by excluding debris and quadrants are drawn to gain four distinct sub-populations.

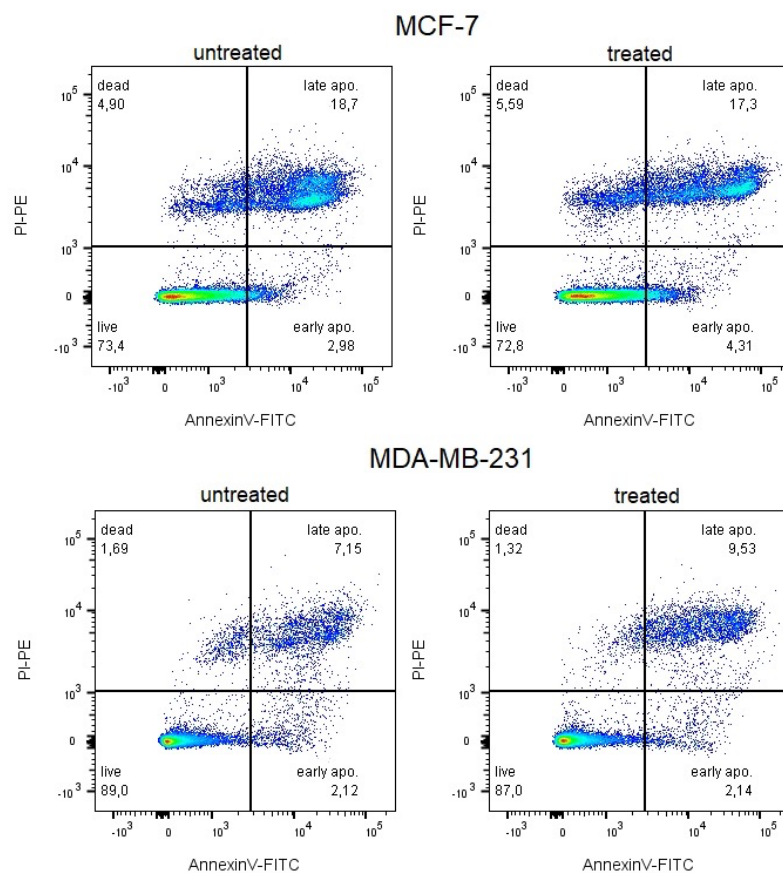


Figure S4: Representative plot of AnnexinV/PI assay in MCF-7 and MDA-MB-231 cells. The AnnexinV versus PI plot shows the four populations, which are dead cells, late apoptotic cells, early apoptotic cells, and live cells. The experiments were performed at least three times and representative data is presented.